Published in final edited form as:

Biochemistry. 2021 May 18; 60(19): 1485–1497. doi:10.1021/acs.biochem.1c00062.

RNA editing of the human DNA glycosylase NEIL1 alters its removal of 5-hydroxyuracil lesions in DNA

Jongchan Yeo,

Elizabeth R. Lotsof,

Brittany M. Anderson-Steele,

Sheila S. David

Department of Chemistry, University of California, Davis, One Shields Avenue, Davis, CA 95616

Abstract

Editing of the pre-mRNA of the DNA repair glycosylase NEIL1 results in substitution of Lys with Arg in the lesion recognition loop of the enzyme. Unedited (K242, UE) NEIL removes thymine glycol lesions in DNA ~30 times faster than edited (R242, Ed) NEIL1. Herein, we evaluated recognition and excision mediated by UE and Ed NEIL1 of 5-hydroxyuracil (5-OHU), a highly mutagenic lesion formed via oxidation of cytosine. NEIL1 catalyzed low levels of 5-OHU excision in single-stranded DNA, bubble and bulge DNA contexts and in duplex DNA base paired with A. Removal of 5-OHU in base-pairs with G, T and C was found to be faster and proceed to a higher overall extent with UE over Ed NEIL1. In addition, the presence of mismatches adjacent to 5-OHU magnified the hampered activity of the Ed isoform. However, Ed NEIL1 was found to exhibit higher affinity for 5-OHU:G and 5-OHU:C duplexes than UE NEIL1. These results suggest that NEIL plays an important role in detecting and capturing 5-OHU lesions in inappropriate contexts, in a manner that does not lead to excision, to prevent mutations and strand breaks. Indeed, inefficient removal of 5-OHU by NEIL1 from 5-OHU:A bps formed during replication would thwart mutagenesis. Notably, non-productive engagement of 5-OHU by Ed NEIL1 suggests 5-OHU repair will be reduced under cellular conditions, such as inflammation, that increase NEIL1 RNA editing. Tipping the balance between the two NEIL isoforms may be a significant factor leading to genome instability.

Graphical Abstract

Corresponding Author: Sheila S. David – Department of Chemistry, University of California, Davis, One Shields Avenue, Davis, California 95616, United States; Phone: (530) 752- 4280; ssdavid@ucdavis.edu.

Author Contributions

J.Y. and S.S.D designed the study. J.Y., B.A.S., and E.R.L. performed the experiments. The manuscript was written through contributions of all authors. All authors* have given approval to the final version of the manuscript. *Note, J.Y. passed-away on June 12, 2020. This work is largely based on work in his Ph.D. thesis, University of California, Davis, 2012. S.S.D., B.A.S. and E.R.L. dedicate this manuscript in fond memory to Jongchan.

The Supporting Information is available free of charge at https://pubs.acs.org/doi/10.1021/acs.biochem.XXXX

Representative production curve and kinetic parameter for 5-OHU removal from a 5-OHU:G-containing duplex by Ed and UE NEIL1 at higher two-fold increased concentration; Representative production curves and kinetic parameters for 5-OHU removal at different buffer NaCl concentrations.

Accession IDs

NEIL1: UniProtKB Q96F14

The authors declare no competing financial interest.

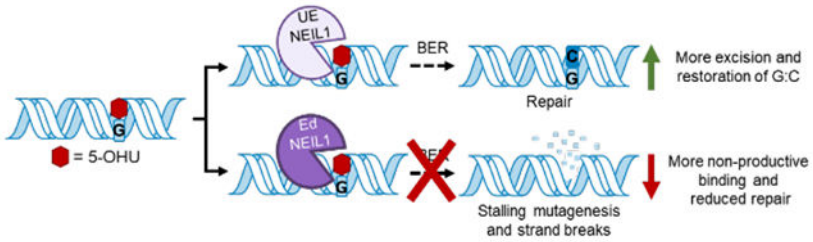

INTRODUCTION

The proper coding of DNA nucleobases may be eroded by oxidative modifications as a consequence of reactive oxygen and nitrogen species (RONS) produced endogenously due to metabolism and inflammatory responses, or exogenously due to ionizing radiation and exposure to environmental chemicals.[1] RONS lead to formation of many oxidatively modified DNA bases, such as 8-oxo-7,8-dihydroguanine (OG), thymine glycol (Tg), 5-hydroxyuracil (5-OHU), formamidopyrimdines (FapyG and FapyA) and the hydantoin lesions, spiroiminodihydantoin (Sp) and guanidinohydantoin (Gh) (Figure 1).[2,3] Arguably, the most common, and well-studied is the oxidized guanine product, OG, that mediates G to T transversion mutations due to its mimicry of T during DNA replication.[3,4] Similarly, 5-OHU arises from the oxidation of cytosine followed by deamination, thereby mediating C to T transition mutations via replicative insertion of A.[5–7] Lesions such as Tg are less mutagenic but are detrimental due to the ability to block DNA replication machinery, which may potentially lead to DNA strand breaks.[8,9] Accumulation of DNA breaks and mutations associated with oxidative stress erodes the integrity of the genome and sets the stage for deleterious disease outcomes.[10]

Oxidized base repair in mammalian cells is mediated primarily by the base-excision repair (BER) pathway. Lesion specific DNA glycosylases recognize the oxidatively damaged DNA bases and initiate BER by catalyzing N-glycosidic bond hydrolysis of the damaged nucleotide.[11] The NEIL1 glycosylase (UniProtKB Q96F14) has been shown to catalyze the removal of a wide variety of oxidized bases including Gh, Sp, FapyG, FapyA and 5-OHU (Figure 1).[12–16] Of note, NEIL1 does not effectively remove OG.[13,17] The NEIL1 glycosylase is a bifunctional glycosylase that possesses an associated AP-lyase (β/δ-elimination) activity; the β/δ- elimination leaves 3’ and 5’ phosphate DNA ends. The 3’ phosphate is removed by polynucleotide kinase (PNK) to generate 3’ OH. The gap is then filled by DNA polymerase β and sealed by DNA ligase III.[16,18]

NEIL1 has been implicated to participate in replication and transcription in part due to its ability to excise lesions in non-duplex contexts such as single stranded (ss), bubble, bulge and G-quadruplex DNA.[10,19,20] In addition, NEIL1 expression is higher in S-phase and the disordered C-terminus of NEIL1 has been shown to interact with DNA replication proteins including replication protein A (RPA),[21] proliferating cell nuclear antigen (PCNA),[22] replication factor C (RF-C),[23] flap endonuclease 1 (FEN1),[24] and Werner RecQ helicase (WRN).[25] NEIL1 has been shown to bind to 5-OHU in replication-mimicking ss and bubble DNA but does not catalyze 5-OHU removal in these contexts.[26] NEIL1 also has been

shown to bind 5-OHU in RPA-coated ssDNA templates and inhibit DNA synthesis by DNA pol δ.[20,26] In these instances, NEIL1 competed for binding with pol δ to prevent strand elongation. [20,26] Based on these observations, Mitra, Hegde and co-workers have proposed a "cowcatcher" model for NEIL1-mediated pre-replication BER where nonproductive binding of NEIL1 to 5-OHU in ssDNA stalls the replication fork to allow for fork regression, and reformation of a duplex substrate for NEIL1-mediated repair. [20,26]

A property distinct for NEIL1 from other BER glycosylases is the presence of two isoforms due to editing of the NEIL1 pre-mRNA by the adenosine deaminase acting on RNA (ADAR1).[28] We previously demonstrated that adenosine at position 725 of the NEIL1 pre-mRNA is converted to inosine by ADAR1-catalyzed deamination.[28] During translation, inosine codes like a guanosine resulting in recoding of edited NEIL1 mRNA to place an arginine (R) at position 242 opposed to the originally coded lysine (K).[28] Based on sequence alignments with the bacterial homolog Fpg and the NEIL1 X-ray structures, the Lys or Arg residue is located within the proposed lesion recognition loop.[28–30] Our laboratory has shown that this single amino acid change in NEIL1 dramatically alters the glycosylase activity in a lesion-specific manner.[28] The unedited (K242, UE) NEIL1 removes the Tg lesion ~30-40 fold faster than edited (R242, Ed) NEIL. In contrast, Ed NEIL1 exhibits ~3-4 fold greater activity towards the removal of the hydantoin lesions, Gh and Sp, than the UE enzyme.[28] Further analysis with K242A, K242E, and K242Q showed significantly reduced rate of Tg lesion removal while the lyase activity was unaffected supporting the importance of residue 242 on catalysis of the base excision step by NEIL1.[30] Electrophoretic mobility shift assays (EMSA) utilizing oligonucleotides containing non-cleavable synthetic 2'-fluorothymidine glycol (FTg) and 2'F-guanidinohydantoin (FGh) showed that the affinity for the lesions was similar between the two isoforms.[31,32] This suggests that the difference in lesion processing is not related to lesion binding affinity, but rather to a kinetic step in lesion processing. This idea is also supported by X-ray crystal structures of Ed and UE NEIL1 bound to a Tg containing duplex where the Lys or Arg 242 side chain appears to be positioned for making direct contacts the damaged base.[30]

Herein, we evaluated 5-OHU lesion removal by Ed and UE NEIL1. Factors such as DNA context, opposite base dependence and salt concentration were evaluated. We also evaluated the impact of mismatches flanking 5-OHU to provide for local destabilization. Relative affinities of Ed and UE NEIL1 with 5-OHU:G and 5-OHU:C duplexes were determined to correlate the relationship of affinity with efficiency of base excision. Our studies revealed preferential excision of 5-OHU by UE NEIL1. The overall extent of lesion removed by both Ed and UE NEIL1 was significantly reduced when 5-OHU was located in ssDNA, bulge and bubble DNA contexts, and also when base-paired with A. These results further elaborate the "cowcatcher" hypothesis that implies a role for NEIL1 to capture but not remove lesions prior to DNA replication. The lack of activity of NEIL1 toward removal of 5-OHU in post-replicative 5-OHU:A bps also suggests a more global role of NEIL1 non-productive binding to prevent mutagenic repair. In duplex contexts where 5-OHU is paired with G, and C, UE NEIL1 shows a faster rate of excision, and also a higher extent of substrate converted to product. This suggests that ADAR1 expression and subsequent NEIL1 mRNA editing may impact mutagenesis and toxicity ensuing from oxidation of cytosine.

MATERIALS AND METHODS

General Material and Methods

The oligonucleotide containing 5-hydroxyuracil (5-OHU) was purchased from Midland Reagents, and all other oligonucleotides were purchased from IDT. The oligonucleotides were purified via a Beckman Gold Nouveau HPLC with a Dionex DNAPac PA-100 column. Radiolabeling was performed with [γ-^{32}P]-ATP purchased from Perkin Elmer. T4 polynucleotide kinase was obtained from New England BioLabs. Pharmacia Microspin G-50 columns were utilized to purify labelled oligonucleotides. Both isoforms of NEIL1 (Uniprot Q96F14) were overexpressed using a pET30a plasmid containing the gene encoding either K242 or R242 NEIL1 in the Rosetta (DE3) pLysS cell strains (Novagen). Enzyme purification was performed with an AKTA FPLC (GE Life Sciences). Buffers were made using distilled, deionized water from a Milli-Q PF water system. A Typhoon 9400 phosphor imager was utilized for storage phosphor autoradiography and gel images were quantitated using ImageQuaNT 5.4 software. The resulting data was fit using GraFit 5.0.2 software to determine rate constants and associated amplitudes. All other chemicals utilized in these experiments were purchased from Fisher Scientific, Millipore Sigma, or VWR and used without further purification.

Substrate DNA Preparation

All oligonucleotide sequences used for these experiments are shown in Figure 2. The 5-OHU containing oligonucleotide was radiolabeled at the 5' end with [γ-^{32}P]-ATP using T4 polynucleotide kinase at 37°C, after which excess [γ-^{32}P]-ATP was removed using a Pharmacia Microspin G-50 spin column. Appropriate amounts of un-labeled 5-OHU-containing oligonucleotide was added to the labeled strand for the appropriate concentration needed with 5% (maximally) labeled DNA for glycosylase assays. The 5-OHU strand was mixed with the appropriate complement (in 20% excess) to form the various substrates (Figure 2), followed by incubation at 90 °C for 5 min and slowly cooling to 4 °C in annealing buffer (20 mM Tris-HCl pH 7.6, 10 mM EDTA, and 150 mM NaCl).

Enzyme Purification

C-terminally His-tagged edited (R242) and unedited (K242) NEIL1 were purified as described previously.[13] Protein concentration was determined by the Bradford Assay using BSA as the standard. Purified enzymes were stored in liquid nitrogen in storage buffer (20 mM HEPES pH 7.6, 25% glycerol, 150 mM NaCl). For these variants, the active enzyme concentration was determined as described previously,[13] and the concentrations reported are active rather than total protein concentration.

In order to prepare C-terminal truncated, inactive (Δ56 K54L) variants, the codon for Leu at position 54 and a stop codon at position 335 were introduced into the R242 and K242 NEIL1 genes using Quikchange® II XL Site-Directed Mutagenesis Kit (Stratagene). The truncated proteins were expressed in Rosetta (DE3) pLysS cell strain, with a purification strategy similar to the WT enzymes.[28] Briefly, the proteins were purified using a HiTrap™ SP Sepharose High Performance ion exchange column (GE Healthcare) equilibrated with Buffer A [20 mM HEPES pH 7.6, 100 mM NaCl, 10% glycerol, 5 mM β-mercaptoethanol].

The NEIL proteins were eluted with Buffer B [Buffer A containing 1 M NaCl] using a step gradient to increase the concentration of Buffer B (15%, 30%, 50%, 75%, and 100%). The samples were loaded onto a HiTrap™ Heparin column (GE Healthcare) equilibrated with Buffer A and eluted with the same step gradient of Buffer B as used above. Δ56 K54L R242 and K242 NEIL1 enzymes eluted between 75% and 100% Buffer B. Purified enzymes were stored at −80°C in storage buffer (above). The "active" fraction of inactive K54L NEIL1 was estimated based on the ability to bind stoichiometrically to a DNA duplex containing an abasic site mimic, THF, opposite C.[33] Total concentrations determined by Bradford assay were corrected using these active fractions.

Glycosylase Assay

The glycosylase activity of NEIL1 was evaluated under single-turnover conditions ([Enzyme]>[DNA]) to provide the rate constant (k_g) as previously reported.[13,34] Briefly, 20 nM of 5-OHU-containing DNA was incubated at 37°C with 200 nM of active NEIL1 isoform in glycosylase assay buffer (20 mM Tris-HCl pH 7.6, 10 mM EDTA, 0.1 mg/mL BSA and various NaCl concentrations). Aliquots were removed from the reaction mixture at various time points and quenched in NaOH at 90°C. Data analysis was performed using ImageQuaNT software version 5.4 for quantification and Grafit software version 5.0.2 for fitting. The resulting production curves were fitted with one or two exponential equations, $[P]_t = A_0[1\text{-}\exp(-k_g t)]$ and $[P]_t = A_0(1\text{-}\exp(-k_g' t)) + B_0(1\text{-}\exp(-k_g'' t)$, respectively, to determine the relevant rates constants to describe the glycosylase steps (k_g, k_g', k_g''). The overall extent of 5-OHU removed (%) was determined by dividing A_0 by 20, which is the total concentration of substrate, and multiplying by 100.

Electrophoretic Mobility Shift Assays (EMSA)

Due to the low concentrations required, only labeled DNA was used in EMSA. The 5'-OH end of 5-OHU-containing strand was radiolabeled with [γ-^{32}P] ATP and annealed to an excess (20%) of the complementary strand. In these experiments, the DNA concentration was estimated as an upper limit assuming no loss of labeled DNA after removal of the excess [γ-^{32}P] ATP to insure that [DNA] < K_d. Enzyme solutions with various concentrations were prepared by diluting enzyme stock solutions with dilution buffer (20 mM Tris pH 7.6, 10 mM EDTA, 20% glycerol) on ice. Labeled DNA duplex was mixed with enzyme solution to give 10 pM of labeled duplex DNA, 10% glycerol, 0.1 mg/mL BSA, 20 mM Tris pH 7.6, 150 mM NaCl, and 1 mM EDTA. All mixtures were immediately incubated at 25°C for 30 minutes. Samples were electrophoresed on a 6% native polyacrylamide gel with 0.5X TBE buffer at 250 V for 10 minutes followed by 120V for two hours. Dried gels were exposed to storage phosphor screens overnight. Quantitation of the storage phosphor autoradiogram provide plots of %bound duplex as a function of [Enzyme] that was fit to a one site binding equation using Grafit software version 5.0.2 to determine the relative dissociation constants.

RESULTS

Context dependent removal of 5-OHU by Ed and UE NEIL1

Previous studies that identified 5-OHU as a substrate of NEIL1 used only Ed NEIL1 (R242).[14,17,35] To reveal potential differences due to NEIL1 recoding, we evaluated 5-OHU removal by Ed and UE NEIL (K242) within duplex DNA, ssDNA, bulge, and bubble DNA contexts. The lesion-containing sequences (Figure 2) were identical to those previously used to evaluate removal of the Gh and Sp lesions by Ed NEIL1.[19] In the duplex substrate, C was placed opposite 5-OHU for direct comparison to the hydantoin lesions. The general method entailed end-labeling the lesion-containing strand of the substrate with [γ-^{32}P]-ATP and determining the extent of strand scission as the lesion site.[13] Reactions were performed by incubating NEIL1 in excess over duplex DNA at 37°C for 60 min followed by NaOH quenching to ensure strand scission at all abasic sites formed by NEIL1. These experiments revealed that both NEIL1 isoforms excise 5-OHU, to some extent, from all DNA contexts. Notably, no significant differences in amounts of overall 5-OHU removal between the isoforms was observed under these conditions. The percentage of NEIL1 catalyzed excision of 5-OHU in ss, bulge, and bubble DNA contexts was less than 20%; however, the amount of the 5-OHU:C duplex substrate processed by Ed and UE NEIL1 was considerably higher (~80%) than the other substrate contexts (Figure 3A and B). Notably, even the 5-OHU:C duplex substrate was not completely converted to product despite enzyme being in excess. In addition, doubling the concentration of NEIL1 enzyme did not increase the amount of NEIL1-dependent excision (Figure S1 and Table S1). These initial experiments revealed low extents of 5-OHU removal by both Ed and UE NEIL1 in non-duplex contexts, like ss DNA, similar to previous work with the Ed isoform.[26]

The impact of the base opposite 5-OHU in duplex DNA on its removal by the NEIL isoforms was evaluated under the same conditions. Since 5-OHU derives from an oxidized C, an expected biological context would be opposite G. *In vitro* studies with DNA polymerases have shown incorporation of A,G, C and T opposite 5-OHU;[6,27,36] though *in vivo* mutagenesis experiments suggest A is most commonly inserted opposite 5-OHU.[7,37] The extents of 5-OHU removed by Ed and UE NEIL1 from the 5-OHU:Y duplex substrate (Y = A, T, G and C) after 60 minutes are shown in Figure 3C. Notably, incomplete and reduced levels of 5-OHU removed were observed with both NEIL1 isoforms in the DNA duplex substrates paired with A, T, or G relative to C (Figure 3C). 5-OHU removal from the 5-OHU:A-containing duplex by Ed and UE NEIL1 was found to be less than 15% of the total substrate. Interestingly, the extent of 5-OHU removed from 5-OHU:G and 5-OHU:T-containing duplexes by Ed NEIL1 was significantly reduced compared to UE NEIL1. Specifically, the extent of 5-OHU removal by UE NEIL1 opposite G and T was approximately 60% and 70%, respectively, while the corresponding extents of removal were approximately 25% for the Ed enzyme for both substrates (Figure 3C and Table 1). Overall, these assays show that the 5-OHU:C duplex was the best substrate context for Ed and UE NEIL1. 5-OHU is removed more efficiently by UE NEIL1 when paired with G or T, but there was no difference in 5-OHU removal between the two isoforms when the lesion was paired with C or A.

Kinetics of NEIL1 5-OHU excision in different base pair contexts

The qualitative analysis of the opposite base dependence of 5-OHU removal by Ed and UE NEIL1 (Figure 3C) prompted an in-depth kinetic analysis of the glycosylase activity on these substrates (Figure 4, Table 1). These experiments were performed under single-turnover conditions to isolate the intrinsic rate of base excision, due to the slow turnover of NEIL1, similar to that previously observed with Tg, Gh, and Sp lesion-containing substrates.[13,28] A feature distinct from that with Tg, Gh, and Sp substrates that emerged in fitting of the production curves for 5-OHU removal was significantly better fitting of the data to a two-exponential equation ($[P]_t = A_0(1\text{-}\exp(-k_g' t)) + B_0(1\text{-}\exp(-k_g'' t))$). This equation describes an initial large rate constant (k_g') and associated amplitude (A_0) and a second smaller rate constant (k_g'') and associated amplitude (B_0). In contrast, under similar conditions with NEIL1 and Gh, Sp, and Tg- containing substrates, production curves fit well to a single exponential equation $[P]_t = A_0(1\text{-}\exp(-k_g t))$ with a single rate constant (k_g).[13,28] Generally, the amplitude associated with k_g' were found to be small, and the experimental limitations provided a lower-limit for the rate constant k_g' (>2 min^{-1}); for example, with the DNA duplexes containing 5-OHU paired opposite G, T, and C, most of the product formed is associated with the slower process (k_g''). Table 1 lists the rate constants obtained from the glycosylase assays for both isoforms of NEIL1 and 5-OHU in the four duplex DNA contexts.

Both the rate and the overall extent of 5-OHU removed by Ed and UE NEIL1 was affected by the identity of the opposing base. With the 5-OHU:G substrate (Figure 4A, Table 1), the rate constants for k_g'' were similar for both isoforms (0.22 and 0.11 min^{-1} for Ed and UE, respectively); however, the overall extent of base excised was significant greater with the UE enzyme (24% versus 68% for Ed and UE, respectively). Similar results were obtained with the 5-OHU:T substrate (Figure 4B, Table 1). In contrast, with the 5-OHU:A substrate, the low levels of 5-OHU removed (<15%) was associated with the larger rate constant k_g' (Figure 4C, Table 1). With 5-OHU paired to C (Figure 4D), the UE enzyme was found to remove 5-OHU considerably more efficiently with k_g'' for UE (1.8 min^{-1}) being six times greater than Ed NEIL1 (0.33 min^{-1}) (Table 1). Overall, these results show that 5-OHU was more efficiently removed by UE than Ed NEIL1, as evidenced by an increased rate for removal with the 5-OHU:C substrate and greater overall extents of base excised with the 5-OHU:G and 5-OHU:T substrates.

The effect of adjacent mismatches on the removal of 5-OHU by NEIL1

5-OHU has been reported to base pair with all four natural bases with 5-OHU:G and 5-OHU:C as the most and least stable bps, respectively.[6,27] Since the best substrates for NEIL1, such as Gh and Sp, are helix destabilizing,[13,38] we have previously suggested that NEIL1 may have higher affinity and activity to lesions that locally disrupt the DNA duplex stability. The lower stability of the 5-OHU:C bp may contribute to the more efficient removal activity of 5-OHU by NEIL1 than in other base-pairing contexts. In order to further evaluate the influence of local stability on 5-OHU excision, a destabilizing C-C or T-T mismatch was introduced to either the 5’ or 3’ side of the 5-OHU:C base pair. Surprisingly, our results show that the presence of adjacent mismatches reduced 5-OHU excision activity with Ed NEIL1 (Figure 5A) and UE NEIL1 (Figure 5B). Notably, with both enzymes, the

amplitude associated with the faster removal process (k_g') in the two-exponential fit was reduced slightly (~1.5-2-fold). The presence of the C-C mismatch 3' to 5-OHU did not significantly reduce the overall extent of 5-OHU removal for either enzyme but reduced the rate constant (k_g") 5-fold for Ed and ~6-fold for UE. The 5' C-C mismatch had a more dramatic effect on the 5-OHU removal by both isoforms. The total extent of reaction on the 5' mismatch substrate relative to the non-mismatch duplex was reduced ~2.5-fold, and the rate constant k_g" by 10-fold for the Ed enzyme. In contrast with the UE enzyme, the overall extent of 5-OHU removed was slightly reduced whereas the rate constant k_g" was reduced significantly (50-fold) (Table 2). The UE isoform processed both the 3' and 5' mismatch more efficiently in terms of the reaction rate and the total amount of 5-OHU excised (Table 2) compared to Ed NEIL1. Specifically, the UE NEIL1 cleaved 5-OHU adjacent to a 3' T-T mismatch 5-fold faster (k_g") than the Ed with slightly higher percent completion. In the case of the 5' C-C mismatch duplex, UE NEIL1 removed the 5-OHU with only a slightly higher rate, but to a significantly greater extent of completion (2.5-fold).

Influence of NaCl concentration on 5-OHU removal in duplex substrates by NEIL1

In all contexts and base pairs, the 5-OHU lesion substrate was never fully converted to product despite NEIL1 being in excess. DNA binding proteins often have different optimal salt concentrations and different "salt sensitivities" for binding.[39] Typical buffer salt conditions that we have used contain 150 mM NaCl, and therefore the low percent of reaction completion consistently observed may be a consequence of altered protein-DNA interactions at this particular ionic strength. To assess the impact of ionic strength, the excision of 5-OHU opposite C and G by the two NEIL1 isoforms was evaluated at 60 and 150 mM NaCl under single turnover (STO) conditions. Notably, the observed rate constants (k_g") at the two different NaCl concentrations were similar and a greater change was observed in the amplitudes of the associated rates, and the overall extent of substrate processed (Table S2). For the cleavage of 5-OHU:G substrates, the Ed enzyme was more sensitive to salt concentration. Ed NEIL1 was able to complete the reaction up to 60% at 60 mM NaCl compared to only 25% completion under the higher salt conditions (Figure S2A). In contrast to the edited enzyme, the activity of UE NEIL1 was largely independent of salt concentration with results showing more constant activities at 55-60% completion (Figure S2B). The activity of 5-OHU removal with 5-OHU:C by both NEIL1 isoforms showed similar trends (Table S2). Ed NEIL1 had a reaction completion of 55% at 150 mM NaCl that increased to 70% at 60 mM NaCl (Figure S2C). The reaction with UE NEIL1 had a similar overall level of 5-OHU removal at both 60 and 150 mM NaCl with a maximum endpoint of 85% (Figure S2D).

Recognition of 5-OHU base pairs by NEIL1

Electrophoretic mobility shift assays (EMSA) were used to evaluate the relative dissociation constants (K_d) of Ed and UE NEIL1 with the 5-OHU:C and 5-OHU:G-containing duplexes. To prevent 5-OHU excision, an inactivating mutation (K54L) was introduced into a C-terminal truncated form Ed and UE NEIL1 (Δ56). The truncated form of NEIL1 improves the quality of gel images, presumably due to the absence of the unstructured C-terminus of NEIL1.[29,40] Increasing amounts of Ed or UE K54L Δ56 NEIL1 was incubated with the 5'-labeled 5-OHU:C or 5-OHU:G DNA duplex, followed by analysis of the samples

by native gel electrophoresis to separate free from bound DNA duplex.[32] The EMSA demonstrated that both 5-OHU:C and 5-OHU:G duplexes were bound completely (nearly 100%) by both Ed and UE NEIL1 (Figure 6A and 6B). Ed and UE NEIL1 exhibited a 10-fold higher affinity with the 5-OHU:C- than 5-OHU:G-containing duplex (Table 3). Unexpectedly, the UE enzyme exhibited 2~3-fold lower affinity compared to the Ed enzyme for both 5-OHU substrates. Notably, these binding results are opposite from the observed trends in the 5-OHU removal by the two isoforms. The UE isoform of NEIL1 removed 5-OHU with a larger rate constant and generally *higher* levels of overall levels of completion compared to the Ed isoform, yet UE NEIL1 demonstrated *reduced affinity* for the substrate. These patterns in binding and catalysis between the two isoforms indicate that the observed differences in the intrinsic rate of glycosidic bond cleavage and extents of 5-OHU removed are not simply due to overall differences in DNA binding and point to more subtle differences in lesion engagement within lesion binding site(s).

DISCUSSION

Base excision by BER glycosylases provides a mechanism to prevent mutagenesis and toxicity of oxidatively modified DNA bases produced under conditions of oxidative stress. As a highly abundant product of cytosine oxidation and deamination, 5-OHU has emerged as a likely candidate responsible for C to T transitions resulting from oxidative stress.[5,7] In addition to NEIL1, several other human BER glycosylases such as SMUG1, TDG, UNG2 and NTHL1 have been shown to remove 5-OHU and suppress 5-OHU induced mutagenesis.[7,35,41–44] This suggests overlapping and potentially distinct roles for each glycosylase in mediating 5-OHU repair and preventing its mutagenicity. Herein we show that two NEIL1 isoforms, resulting from RNA editing, display distinctly different activities towards 5-OHU removal, which is highly dependent on the DNA context. Our results provide another layer of complexity to an already complex mutagenesis versus repair landscape associated with nucleobase oxidation.

Our results showed that Ed and UE NEIL1 excised 5-OHU to differing extents in bubble, bulge, single-stranded and duplex DNA (Figure 3A and 3B). Notably, a distinct feature that emerged in the analysis of 5-OHU removal was differences in the overall amount of 5-OHU-containing substrate converted to product even after long incubation periods with NEIL1 in excess, and these differences in extent of removal were dependent on both 5-OHU DNA context and NEIL1 isoform. In the case of single-stranded, bubble and bulge contexts, the amount of 5-OHU removed was relatively low (< 20%) and similar for both isoforms. With the notable exception of 5-OHU:A bps, Ed and UE NEIL1 mediated more efficient removal of 5-OHU in duplex DNA consistent with previous reports for Ed NEIL1.[17,45] Inefficient removal of 5-OHU by NEIL1 in ssDNA, and its ability to stall replication, led Mitra and co-workers to propose that NEIL1 acts as a “cow catcher” to capture lesions prior to replication. [20,26] In this model, non-productive binding of NEIL1 to 5-OHU in single-stranded DNA facilitates stalling of the replication machinery and fork regression that allows for reannealing of the duplex for NEIL1-initiated BER.

The dramatic influence of the opposite base on NEIL1 excision of 5-OHU in duplex DNA further elaborates how binding and stalled lesion removal activity of NEIL1 in

specific contexts prevents mutations associated with 5-OHU. The excision of 5-OHU by both isoforms was found to be highly dependent on the opposite base, with the overall preference of C > T, G > A. Since 5-OHU arises from oxidative deamination of C, formation in duplex DNA would be opposite G; however, upon replication, insertion of A is the most prevalent based on *in vivo* mutagenesis experiments.[3,7] Strikingly, very low levels of excision of 5-OHU from 5-OHU:A was observed with both Ed and UE (<15%). The inability of both NEIL1 isoforms to completely remove 5-OHU from 5-OHU:A bps in duplex DNA is distinct from that observed previously with the hydantoin lesions, Gh, and Sp; indeed, in the same sequence and under the same conditions, Gh and Sp are removed rapidly and completely in all duplex substrate base pairing contexts by both isoforms.[13,19] Notably, this low NEIL1 activity on 5-OHU:A would provide a mechanism to prevent pro-mutagenic removal of 5-OHU. This is highly analogous to OGG1 that exhibits poor activity towards removal of OG from OG:A bps.[16,46] Mutations mediated by OG:A base-pairs are prevented by the adenine glycosylase MUTYH that removes the inappropriate placed A's.[16] However, a glycosylase capable of removing A opposite 5-OHU has yet to be identified. This implies an expanded "cow-catcher" role of NEIL1 to capture the 5-OHU lesions formed post-replication in inappropriate contexts to thwart propagation of deleterious DNA mutations.

A surprising result in the analysis of the opposite base dependence was the finding that both NEIL1 isoforms excised 5-OHU most efficiently opposite C (Figure 3C and 4). Ed and UE NEIL1 also exhibited higher affinity for duplex DNA containing 5-OHU:C relative to 5-OHU:G bps (Figure 6 and Table 3). Mammalian polymerases have been found to insert A, G, and T opposite 5-OHU with different efficiencies;[47] however, there is no evidence for C mispairing *in vivo* with 5-OHU. Calculations indicated that the C within a 5-OHU:C bps twists out of plane due to repulsive interactions of the O4 of 5-OHU and the cytosine amino group.[27] The bp propeller twisting would disrupt local base-stacking and provides a rationale for the lower stability of the 5-OHU:C bp.[27] The distorted and destabilized 5-OHU:C bp may be a factor that aids Ed and UE NEIL1 in extruding 5-OHU from the DNA helix. Moreover, the crystal structure of Ed and UE NEIL1 bound to a Tg:C containing duplex shows favorable contacts between orphaned C and Arg 118 (Figure 7A).[30] The interaction of this Arg with C also likely contributes significantly to the enhanced cleavage of 5-OHU across from C by NEIL1, and the opposite base is likely an important factor used by NEIL1 to select damaged bases in proper contexts for excision. Indeed, oxidized guanine derivatives, such as Gh, Sp or FapyG, where C would be the natural bp context, are all good substrates for NEIL1.[13,15] The sensing of "C" by NEIL1 via the interaction with Arg 118 may allow for more facile lesion bp recognition, nucleotide flipping and effective engagement of the lesion within the active site to effect cleavage. Thus, the opposite base influence is likely a key fidelity mechanism of NEIL1 to identify specific lesions for binding versus cleavage in different contexts.

The preference of NEIL1 for removal of lesions in canonical duplex DNA contexts was further supported by analysis of the impact of mismatches flanking 5-OHU:C bps on the extent and efficiency of 5-OHU excision (Figure 5 and Table 2). We expected instability surrounding the 5-OHU:C bp to enhance 5-OHU excision. However, the presence of a C:C or T:T mismatch 5' or 3' to 5-OHU, respectively, reduced the ability of both NEIL1

isoforms to excise 5-OHU. This was more detrimental for both Ed and UE NEIL1 when a 5' mismatch was present compared to a 3' mismatch. Upon examination of the NEIL1-lesion crystal structure,[30] NEIL1 makes additional contacts to the 3' side relative to the lesion compared to the 5' side (Figure 7B). Seven residues, K54, R78, Q130, R133, Q168, N176, and R277, make contact with the phosphodiester backbone 3' to the Tg on the Tg-containing strand, while only three contacts, N176, Y263, and T278, are observed on the 5' side. The additional contact on the 3' side may be responsible for the slightly better excision noted with the 3' mismatch relative to the 5' mismatch. Overall, UE NEIL1 excised 5-OHU with the 5' or 3' mismatch more efficiently compared to Ed NEIL1, and the superior activity in terms of rate and extent of 5-OHU removed with UE NEIL1 is exaggerated by the presence of the mismatch. The presence of a mismatch adjacent to the 5-OHU:C pair, which is already helix distorting,[27] may generate a small bubble structure where NEIL1 exhibits poor excision (Figure 3B). The reduced activity with the presence of an adjacent mismatch supports the notion that NEIL1 requires canonical B-form duplex DNA for efficient excision, and that phosphodiester contacts in duplex DNA may aid in initial lesion recognition, nucleotide flipping and *proper* active site placement to support catalysis of base excision. Indeed, this may provide a useful mechanism to prevent inappropriate excision by NEIL1 in non-standard contexts, such as those present in replication or transcription intermediates.

UE NEIL1 excised 5-OHU to a greater extent and more rapidly than Ed NEIL1 in several substrate contexts. We previously showed that UE NEIL1 excised Tg, which has structural similarities to 5-OHU, 30 to 40-fold faster than Ed NEIL1.[28] A mechanistic rationale for enhanced removal of Tg by UE NEIL1 was provided by computational studies and X-ray crystal structures of UE and Ed NEIL1 bound to Tg containing DNA.[30] In the Tg bound structure, the flexible loop containing Lys or Arg 242 was observed to adopt a distinct conformation providing a direct interaction with the everted Tg nucleobase (Figure 7C). A direct contact of the Lys or Arg of UE or Ed NEIL1 with N3 of Tg would be unfavorable if N3 were protonated suggesting that the Arg or Lys 242 interaction may promote a keto-enol tautomerization of Tg (Figure 8A) within the active site that enhances its excision.[30] Computational experiments provided support for an enzyme-mediated tautomerization hypothesis.[30] A compelling feature of this mechanism is that it explains the higher activity of the UE enzyme for Tg removal since the lower pKa of Lys relative to Arg would allow for the UE enzyme to more readily catalyze Tg base tautomerization.[30] The NEIL1-tautomerization mechanism also provides a rationale for the ability of NEIL1 to differentiate between lesions and canonical bases since the stability of the more readily excised tautomers will be influenced by conjugation and substituents on the base heterocycle.[30] Thymine has a higher-energy barrier for tautomerization compared to Tg due to its aromaticity. Like T, 5-OHU is aromatic, which would be expected to have a higher barrier for tautomerization than Tg. 5-OHU is excised by NEIL1, but not as efficiently as Tg with smaller k_g" values and less then 100% base removed in conditions of excess enzyme. Additionally, we observed smaller difference in rate of removal between UE and Ed isoforms for 5-OHU (e.g. ~6-fold opposite C, Table 1) relative to that observed with Tg (~ 30-40-fold).[28] DFT studies analyzing the stability of keto-enol tautomers in 5,6-substituted uracils revealed that the presence of the OH group on C5 stabilizes the enol tautomer (Figure 8B) via

an intramolecular hydrogen bond between the oxygen on C4 and the OH group on C5.[48] Future computational studies analyzing the relative stability of tautomeric forms of oxidized pyrimidine and purine substrates of NEIL1 would be particularly useful to further elaborate these intriguing mechanistic hypotheses, and the impact of NEIL1 recoding.

The observed impact of NEIL1 recoding on 5-OHU lesion excision and affinity and the influence of bp context along with the observation of biphasic production curves reveal additional complexities of NEIL1 lesion processing that results from non-productive substrate binding (Figure 9). In contrast to results with Gh, Sp, and Tg, production curves of NEIL1 removal of 5-OHU by both isoforms in duplex contexts (Figure 4) are biphasic and exhibit incomplete levels of product formation despite the enzyme being in excess. In these cases, the data fit better to a two-exponential equation, with distinct large and small rates (k_g', k_g") and associated amplitudes (A, B). We suggest that the two rate constants correspond to two distinct processes where the large rate constant (k_g') is associated with 5-OHU removal for the fraction of substrate bound initially in a catalytically competent complex, while the smaller rate constant (k_g") correlates with a slower process due to the 5-OHU lesion being positioned in an alternative orientation that requires a conformational change to place 5-OHU into a catalytically accessible manner in the active site. Additionally, we propose a third population of 5-OHU lesion positioned such that removal is extremely slow by NEIL1 leading to the incomplete levels of product formation in the time-frame monitored (60 min). X-ray crystal structures of the viral ortholog of NEIL1, *Mv* Neil, bound to 5-OHU:G containing duplex DNA shows 5-OHU bound in *syn* and *anti* conformations within the active site.[49] The most recently proposed mechanism for NEIL1 suggests that contact of 242 with N3 of Tg is necessary for catalysis.[30] Rearrangement of the 5-OHU lesion by NEIL1 may be necessary for proper contacts with residue 242 and other critical catalytic residues, like E6. Similarly, STO kinetics with 5-OHU:G with *Mv* Nei1 yielded results that also were best fitted to a two exponential equation that the authors rationalized stems from the two lesion conformations observed in the *Mv* Nei1 structures.[49] Indeed, a variety of X-ray structural studies with OGG1 and MutY have revealed so-called “exo” base binding sites that are distinct from the active site, and these exo-sites are proposed to be a means to capture inappropriate bases to stall and prevent presentation to the active site for excision.[50,51] Additional structural studies of Ed and UE NEIL1 with 5-OHU substrates, in different contexts, would be useful to elaborate these findings and hypotheses.

NEIL1 recoding results in significant differences in amplitudes associated with the two discrete rates and overall extents of 5-OHU removed. This is most dramatically observed with the 5-OHU:G substrate where UE NEIL1 reactions proceeded to an overall end point of ~70% product formed, while with Ed NEIL1 under the same conditions the observed endpoint was only 25% (Figure 4A). The differences in extent of reaction do not seem to be related to intrinsic differences in lesion affinity since Ed K54L Δ56 NEIL1 was found to bind 3-fold *tighter* than UE K54L NEIL1 to the 5-OHU:G duplex (Table 3). Notably, lower salt concentrations enhanced the extent of product formation with Ed NEIL such that reaction completion increased significantly (68%) approaching that observed with UE NEIL (78%). 5-OHU glycosylase reactions with UE NEIL1 are much less sensitive to the NaCl concentration (Figure S2B and S2D). These results suggest that Ed NEIL1 not only binds 5-OHU substrates more tightly but also with a higher fraction in a non-catalytically

competent complex. At lower salt concentrations, ionic interactions of Ed NEIL1 residues with the phosphodiester backbone may aid in forming the catalytic conformation that supports 5-OHU excision, particularly when across from G. Notably, we have previously observed that a cancer-associated variant of MUTYH that alters an intercalating Tyr residue (Y179C MUTYH) exhibits increased sensitivity of the glycosylase activity to higher buffer salt concentration than the WT enzyme.[52,53] Tyr 179 in MUTYH facilitates OG:A lesion extrusion, engagement, and placement into the active site.[52,53] In the absence of the stabilizing Tyr intercalation, MUTYH ionic interactions with the phosphodiester backbone, possible at low salt, but not higher salt concentrations, facilitate the conformational changes needed to support catalysis.[52,53] We suggest that a similar type of phenomenon is occurring here where UE NEIL1 more readily recognizes and engages 5-OHU within its active site, and therefore is less sensitive to buffer salt concentrations compared to Ed NEIL1. The sensitivity of Ed and UE NEIL1 to the presence of mismatches flanking the 5-OHU lesion is also consistent with the importance of interactions of NEIL1 with duplex DNA to remodel and position the lesion within the active site for excision.

NEIL1 recoding results in distinct differences in excision of Tg, Gh, Sp, and 5-OHU by the two isoforms. Consistent with the importance of residue 242, Tg base excision with A242, E242, and Q242 NEIL1 was significantly compromised relative to that with K242 or R242 NEIL1.[30] The reported structures suggest that contact of residue 242 with the Tg lesion, along with E6, promotes Tg tautomerization that facilitates Tg excision (Figure 7C). Our glycosylase kinetics studies show less efficient removal of 5-OHU compared to Tg for both isoforms, and that the UE NEIL1 removes 5-OHU more efficiently and to a higher level of completion than Ed NEIL1. The differences in the efficiency and overall extent of 5-OH removed was also influenced by the opposite base, suggesting that the role of 242 may be more than as a proton donor to promote lesion excision as recently proposed.[30] Such differences would not be expected if lesion excision was solely dependent on the pK_a difference between K and R. The residue at position 242 and other active site residues likely also play important roles in initial lesion sensing, base flipping and alignment of the lesion with catalytic residues to mediate its excision. Notably, structural and computational studies of NEIL1, and its bacterial cousin Fpg, have underscored the importance of the conformational flexibility of the lesion recognition loop in providing the ability of these enzymes to recognize a diverse set of lesions (Figure 7C and 7D).[29,30,54–56] It also should be noted that in the reported structures of Ed and UE NEIL1 with Tg, the loop was considerably disordered consistent with potentially multiple roles of this flexible region in the lesion recognition and excision process. Moreover, the relative impacts of NEIL1 recoding on lesion sensing, extrusion, and engagement versus enhancing lesion lability would be anticipated to be distinctly different due to the structural features of a given NEIL1 lesion substrate. Indeed, such differences may explain why Gh/Sp and FapyG lesion are processed with more efficiency by Ed NEIL1.[28,57]

The lesion-specific activity differences of UE versus Ed NEIL1 suggests that cellular responses to oxidative stress will be impacted by the relative amounts of the two isoforms. Since ADAR1 is induced in T-lymphocytes and macrophages by TNF-α and IFN-γ,[58–60] Ed NEIL1 would be predicted to be the predominant form present under conditions of inflammation. Notably, ADAR1 overexpression and NEIL1 hyper-editing have been

observed in several types of cancer cells.[61–65] The reduced activity of Ed NEIL1 with Tg and 5-OHU suggests that hyper-editing of NEIL1 over prolonged times may alter the types of mutations that accumulate in the genome. In addition, the tight binding, but incomplete excision, mediated by Ed NEIL1 suggests that non-productive binding may also influence downstream DNA damage responses or aid in recruitment of protein partners to regulate NEIL1 excision. NEIL1 has been reported to interact with DNA replication proteins such as RPA, PCNA, Pol δ, FEN-1, RF-C, and WRN.[20–23,25] In the reported studies, interactions with NEIL1 have been observed either in cell-based experiments, via immunoprecipitation isolation, or through using recombinant Ed NEIL1. In several studies, protein partners have been shown to stimulate Ed NEIL1 activity on oxidative DNA damage. For example, PCNA stimulates NEIL1 activity in the removal of 5-OHU in single-stranded DNA structures such as DNA replication forks,[22] and WRN has been shown to stimulate NEIL1 excision from bubble DNA structures.[25] On the other hand, RPA, which coats the ssDNA template at the replication fork, inhibits NEIL1 activity, and such inhibition is a means to regulate the excision of oxidative base damage from primer-template structures.[21] Such regulatory mechanisms would help protect DNA undergoing replication from the mutagenic lesions that arise from oxidative DNA damage, without generating genotoxic and mutagenic AP sites and SSBs. Interactions with protein partners may also be altered by NEIL1 recoding further amplifying lesion-specific differences in activity. In these various ways, ADAR1-mediated NEIL1 recoding may regulate repair under different cellular conditions. On the other hand, NEIL1 recoding induced by cellular stressors or environmental sources may lead to unanticipated genome rewriting and instability.

CONCLUSION

Herein, we have revealed unique features of NEIL1 removal of the 5-OHU base lesion that provide insight into the impact of NEIL1 activity and NEIL1 recoding on oxidative base induced mutagenesis and toxicity. The removal of 5-OHU by NEIL1 isoforms was found to be inefficient in non-canonical substrate contexts supporting the proposed cellular role of NEIL1 as a “cowcatcher” stalling the replication machinery. The lesion capture behavior of NEIL1 is not limited to alternative DNA contexts but is also dependent on the base opposite the lesion. NEIL1 exhibited minimal excision of 5-OHU across from A, which would prevent C to T transversion mutations that would be propagated by 5-OHU removal in this context. Of note, the enhanced excision of 5-OHU from 5-OHU:C bps by both NEIL isoforms is consistent with the observation that the most efficiently removed lesion substrates for NEIL1 are oxidized guanine products like the hydantoin lesions. The differences in activity 5-OHU removal activity with the two NEIL1 isoform further underscores the lesion-specific impact of NEIL1 recoding. While UE NEIL1 overall demonstrated better excision of 5-OHU, the cellular consequences of the differing activity between the two isoforms warrants further investigation. Likely, a cellular balance of Ed and UE NEIL1 is needed to maintain the integrity of the genome, and alterations to cellular levels of Ed and UE could impact the repair response of NEIL1 under conditions of oxidative stress.

Supplementary Material

Refer to Web version on PubMed Central for supplementary material.

Funding Sources

We gratefully acknowledge funding provided by NIH grant RO1 CA090689 and UC Davis.

ABBREVIATIONS

ADAR1	Adenosine deaminase acting on RNA 1
BER	Base Excision Repair
Ed	Edited
Fapy	formamidopyrimdines
FEN-1	Flap endonuclease 1
Fpg	formamidopyrimidine DNA glycosylase
Gh	guanidinohydantoin
IFNγ	interferon γ
NEIL1	Endonuclease VIII like 1
NTHL1	Endonuclease III like 1
PCNA	proliferating cell nuclear antigen
Pol δ	DNA polymerase δ
RF-C	replication factor C
RPA	replication protein A
SMUG1	single-stranded-selective monofuctional uracil glycosylase 1
Sp	spiroiminodihydantoin
TDG	thymine DNA glycosylase
Tg	Thymine glycol
TNFα	tumor necrosis factor α
UE	Unedited
UNG	Uracil N-glycosylase
WRN	Werner syndrome helicase
5-OHU	5-hydoxyuracil

REFERENCES

(1). Lonkar P; Dedon PC Reactive Species and DNA Damage in Chronic Inflammation: Reconciling Chemical Mechanisms and Biological Fates. International Journal of Cancer. John Wiley & Sons, Ltd May 1, 2011, pp 1999–2009. 10.1002/ijc.25815. [PubMed: 21387284]

(2). Cadet J; Davies KJA; Medeiros MH; Di Mascio P; Wagner JR Formation and Repair of Oxidatively Generated Damage in Cellular DNA. Free Radical Biology and Medicine. Elsevier Inc. June 1, 2017, pp 13–34. 10.1016/j.freeradbiomed.2016.12.049. [PubMed: 28057600]

(3). Dutta A; Yang C; Sengupta S; Mitra S; Hegde ML New Paradigms in the Repair of Oxidative Damage in Human Genome: Mechanisms Ensuring Repair of Mutagenic Base Lesions during Replication and Involvement of Accessory Proteins. Cell. Mol. Life Sci 2015, 72 (9), 1679–1698. 10.1007/s00018-014-1820-z. [PubMed: 25575562]

(4). Neeley WL; Essigmann JM Mechanisms of Formation, Genotoxicity, and Mutation of Guanine Oxidation Products. Chemical Research in Toxicology. American Chemical Society April 2006, pp 491–505. 10.1021/tx0600043. [PubMed: 16608160]

(5). Kreutzer DA; Essigmann JM Oxidized, Deaminated Cytosines Are a Source of C → T Transitions in Vivo. Proc. Natl. Acad. Sci. U. S. A 1998, 95 (7), 3578–3582. 10.1073/pnas.95.73578. [PubMed: 9520408]

(6). Thiviyanathan V; Somasunderam A; Volk DE; Gorenstein DG 5-Hydroxyuracil Can Form Stable Base Pairs with All Four Bases in a DNA Duplex. Chem. Commun 2005, No. 3, 400–402. 10.1039/b414474k.

(7). Shinmura K; Kato H; Kawanishi Y; Goto M; Tao H; Yoshimura K; Nakamura S; Misawa K; Sugimura H Defective Repair Capacity of Variant Proteins of the DNA Glycosylase NTHL1 for 5-Hydroxyuracil, an Oxidation Product of Cytosine. Free Radic. Biol. Med 2019, 131, 264–273. 10.1016/jYreeradbiomed.2018.12.010. [PubMed: 30552997]

(8). Johnson RE; Yu SL; Prakash S; Prakash L Yeast DNA Polymerase Zeta (ζ) Is Essential for Error-Free Replication Past Thymine Glycol. Genes Dev. 2003, 17 (1), 77–87. 10.1101/gad.1048303. [PubMed: 12514101]

(9). Kusumoto R; Masutani C; Iwai S; Hanaoka F Translesion Synthesis by Human DNA Polymerase η across Thymine Glycol Lesions. Biochemistry 2002, 41 (19), 6090–6099. 10.1021/bi025549k. [PubMed: 11994004]

(10). Fleming AM; Burrows CJ Formation and Processing of DNA Damage Substrates for the HNEIL Enzymes. Free Radical Biology and Medicine. 2017. 10.1016/j.freeradbiomed.2016.11.030.

(11). David SS; Williams SD Chemistry of Glycosylases and Endonucleases Involved in Base-Excision Repair. Chem. Rev 1998, 98 (3), 1221–1261. 10.1021/cr980321h. [PubMed: 11848931]

(12). Grin IR; Zharkov DO Eukaryotic Endonuclease VIII-Like Proteins: New Components of the Base Excision DNA Repair System. Biochemistry (Moscow). Springer January 16, 2011, pp 80–93. 10.1134/S000629791101010X. [PubMed: 21568842]

(13). Krishnamurthy N; Zhao X; Burrows CJ; David SS Superior Removal of Hydantoin Lesions Relative to Other Oxidized Bases by the Human DNA Glycosylase HNEIL1. Biochemistry 2008, 47 (27), 7137–7146. 10.1021/bi800160s. [PubMed: 18543945]

(14). Bandaru V; Sunkara S; Wallace SS; Bond JP A Novel Human DNA Glycosylase That Removes Oxidative DNA Damage and Is Homologous to Escherichia Coli Endonuclease VIII. DNA Repair (Amst). 2002, 1 (7), 517–529. 10.1016/S1568-7864(02)00036-8. [PubMed: 12509226]

(15). Jaruga P; Birincioglu M; Rosenquist TA; Dizdaroglu M Mouse NEIL1 Protein Is Specific for Excision of 2,6-Diamino-4-Hydroxy-5- Formamidopyrimidine and 4,6-Diamino-5-Formamidopyrimidine from Oxidatively Damaged DNA. Biochemistry 2004, 43 (50), 15909–15914. 10.1021/bi048162l. [PubMed: 15595846]

(16). David SS; O'Shea VL; Kundu S Base-Excision Repair of Oxidative DNA Damage. Nature 2007, 447 (7147), 941–950. 10.1038/nature05978. [PubMed: 17581577]

(17). Hazra TK; Kow YW; Hatahet Z; Imhoff B; Boldogh I; Mokkapati SK; Mitra S; Izumi T Identification and Characterization of a Novel Human DNA Glycosylase for Repair of Cytosine-Derived Lesions. J. Biol. Chem 2002, 277 (34), 30417–30420. 10.1074/jbc.C200355200. [PubMed: 12097317]

(18). Lee AJ; Wallace SS Hide and Seek: How Do DNA Glycosylases Locate Oxidatively Damaged DNA Bases amidst a Sea of Undamaged Bases? Free Radic. Biol. Med 2017, 107 (September 2016), 170–178. 10.1016/j.freeradbiomed.2016.11.024. [PubMed: 27865982]

(19). Zhao X; Krishnamurthy N; Burrows CJ; David SS Mutation versus Repair: NEIL1 Removal of Hydantoin Lesions in Single-Stranded, Bulge, Bubble, and Duplex DNA Contexts. Biochemistry 2010, 49 (8), 1658–1666. 10.1021/bi901852q. [PubMed: 20099873]

(20). Rangaswamy S; Pandey A; Mitra S; Hegde ML Pre-Replicative Repair of Oxidized Bases Maintains Fidelity in Mammalian Genomes: The Cowcatcher Role of NEIL1 DNA Glycosylase. Genes (Basel). 2017, 8 (7). 10.3390/genes8070175.

(21). Theriot CA; Hegde ML; Hazra TK; Mitra S RPA Physically Interacts with the Human DNA Glycosylase NEIL1 to Regulate Excision of Oxidative DNA Base Damage in Primer-Template Structures. DNA Repair (Amst). 2010, 9 (6), 643–652. 10.1016/j.dnarep.2010.02.014. [PubMed: 20338831]

(22). Dou H; Theriot CA; Das A; Hegde ML; Matsumoto Y; Boldogh I; Hazra TK; Bhakat KK; Mitra S Interaction of the Human DNA Glycosylase NEIL1 with Proliferating Cell Nuclear Antigen: The Potential for Replication-Associated Repair of Oxidized Bases in Mammalian Genomes. J. Biol. Chem 2008, 283 (6), 3130–3140. 10.1074/jbc.M709186200. [PubMed: 18032376]

(23). Hegde PM; Dutta A; Sengupta S; Mitra J; Adhikari S; Tomkinson AE; Li GM; Boldogh I; Hazra TK; Mitra S; Hegde ML The C-Terminal Domain (CTD) of Human DNA Glycosylase NEIL1 Is Required for Forming BERosome Repair Complex with DNA Replication Proteins at the Replicating Genome: Dominant Negative Function of the CTD. J. Biol. Chem 2015, 290 (34), 20919–20933. 10.1074/jbc.M115.642918. [PubMed: 26134572]

(24). Hegde ML; Theriot CA; Das A; Hegde PM; Guo Z; Gary RK; Hazra TK; Shen B; Mitra S Physical and Functional Interaction between Human Oxidized Base-Specific DNA Glycosylase NEIL1 and Flap Endonuclease. J. Biol. Chem 2008, 283 (40), 27028–27037. 10.1074/jbc.M802712200. [PubMed: 18662981]

(25). Das A; Boldogh I; Jae WL; Harrigan JA; Hegde ML; Piotrowski J; Pinto NDS; Ramos W; Greenberg MM; Hazra TK; Mitra S; Bohr VA The Human Werner Syndrome Protein Stimulates Repair of Oxidative DNA Base Damage by the DNA Glycosylase NEIL1. J. Biol. Chem 2007, 282 (36), 26591–26602. 10.1074/jbc.M703343200. [PubMed: 17611195]

(26). Hegde ML; Hegde PM; Bellot LJ; Mandal SM; Hazra TK; Li GM; Boldogh I; Tomkinson AE; Mitra S Prereplicative Repair of Oxidized Bases in the Human Genome Is Mediated by NEIL1 DNA Glycosylase Together with Replication Proteins. Proc. Natl. Acad. Sci. U. S. A 2013, 110 (33). 10.1073/pnas.1304231110.

(27). Thiviyanathan V; Somasunderam A; Volk DE; Hazra TK; Mitra S; Gorenstein DG Base-Pairing Properties of the Oxidized Cytosine Derivative, 5-Hydroxy Uracil. Biochem. Biophys. Res. Commun 2008, 366 (3), 752–757. 10.1016/j.bbrc.2007.12.010. [PubMed: 18078807]

(28). Yeo J; Goodman RA; Schirle NT; David SS; Beal PA RNA Editing Changes the Lesion Specificity for the DNA Repair Enzyme NEIL1. Proc. Natl. Acad. Sci. U. S. A 2010, 107 (48), 20715–20719. 10.1073/pnas.1009231107. [PubMed: 21068368]

(29). Doublié S; Bandaru V; Bond JP; Wallace SS The Crystal Structure of Human Endonuclease VIII-like 1 (NEIL1) Reveals a Zincless Finger Motif Required for Glycosylase Activity. Proc. Natl. Acad. Sci. U. S. A 2004, 101 (28), 10284–10289. 10.1073/pnas.0402051101. [PubMed: 15232006]

(30). Zhu C; Lu L; Zhang J; Yue Z; Song J; Zong S; Liu M; Stovicek O; Gao YQ; Yi C Tautomerization-Dependent Recognition and Excision of Oxidation Damage in Base-Excision DNA Repair. Proc. Natl. Acad. Sci. U. S. A 2016, 113 (28), 7792–7797. 10.1073/pnas.1604591113. [PubMed: 27354518]

(31). Cao S; Rogers J; Yeo J; Anderson-Steele B; Ashby J; David SS 2′-Fluorinated Hydantoins as Chemical Biology Tools for Base Excision Repair Glycosylases. ACS Chem. Biol 2020, 15 (4), 915–924. 10.1021/acschembio.9b00923. [PubMed: 32069022]

(32). Onizuka K; Yeo J; David SS; Beal PA NEIL1 Binding to DNA Containing 2′-Fluorothymidine Glycol Stereoisomers and the Effect of Editing. ChemBioChem 2012, 13 (9), 1338–1348. 10.1002/cbic.201200139. [PubMed: 22639086]

(33). Leipold MD; Muller JG; Burrows CJ; David SS Removal of Hydantoin Products of 8-Oxoguanine Oxidation by the Escherichia Coli DNA Repair Enzyme, FPG. Biochemistry 2000, 39 (48), 14984–14992. 10.1021/bi0017982. [PubMed: 11101315]

(34). Porello SL; Leyes AE; David SS Single-Turnover and Pre-Steady-State Kinetics of the Reaction of the Adenine Glycosylase MutY with Mismatch-Containing DNA Substrates. Biochemistry 1998, 37 (42), 14756–14764. 10.1021/bi981594+. [PubMed: 9778350]

(35). Dou H; Mitra S; Hazra TK Repair of Oxidized Bases in DNA Bubble Structures by Human DNA Glycosylases NEIL1 and NEIL2. J. Biol. Chem 2003, 278 (50), 49679–49684. 10.1074/jbc.M308658200. [PubMed: 14522990]

(36). Purmal AA; Kow YW; Wallace SS Major Oxidative Products of Cytosine, 5-Hydroxycytosine and 5-Hydroxyuracil, Exhibit Sequence Context-Dependent Mispairing in Vitro. Nucleic Acids Res 1994, 22 (1), 72–78. 10.1093/nar/22.L72. [PubMed: 8127657]

(37). Charlet-Berguerand N; Feuerhahn S; Kong SE; Ziserman H; Conaway JW; Conaway R; Egly JM RNA Polymerase II Bypass of Oxidative DNA Damage Is Regulated by Transcription Elongation Factors. EMBO J. 2006, 25 (23), 5481–5491. 10.1038/sj.emboj.7601403. [PubMed: 17110932]

(38). Jin Q; Fleming AM; Ding Y; Burrows CJ; White HS Structural Destabilization of DNA Duplexes Containing Single-Base Lesions Investigated by Nanopore Measurements. Biochemistry 2013, 52 (45), 7870–7877. 10.1021/bi4009825. [PubMed: 24128275]

(39). Datta K; LiCata VJ Salt Dependence of DNA Binding by Thermus Aquaticus and Escherichia Coli DNA Polymerases. J. Biol. Chem 2003, 278 (8), 5694–5701. 10.1074/jbc.M208133200. [PubMed: 12466277]

(40). Vik ES; Alseth I; Forsbring M; Helle IH; Morland I; Luna L; Bjørås M; Dalhus B Biochemical Mapping of Human NEIL1 DNA Glycosylase and AP Lyase Activities. DNA Repair (Amst). 2012, 11 (9), 766–773. 10.1016/j.dnarep.2012.07.002. [PubMed: 22858590]

(41). Katafuchi A; Matsuo A; Terato H; Ohyama Y; Ide H Repair of Oxidative Cytosine Damage by DNA Glycosylases. Nucleic Acids Symp. Ser 2003, 3 (1), 269–270. 10.1093/nass/3.1.269.

(42). Masaoka A; Matsubara M; Hasegawa R; Tanaka T; Kurisu S; Terato H; Ohyama Y; Karino N; Matsuda A; Ide H Mammalian 5-Formyluracil-DNA Glycosylase. 2. Role of SMUG1 Uracil-DNA Glycosylase in Repair of 5-Formyluracil and Other Oxidized and Deaminated Base Lesions. Biochemistry 2003, 42 (17), 5003–5012. 10.1021/bi0273213. [PubMed: 12718543]

(43). Kino K; Takao M; Miyazawa H; Hanaoka F A DNA Oligomer Containing 2,2,4-Triamino-5(2H)-Oxazolone Is Incised by Human NEIL1 and NTH1. Mutat. Res. - Fundam. Mol. Mech. Mutagen 2012, 734 (1–2), 73–77. 10.1016/j.mrfmmm.2012.03.007.

(44). Dizdaroglu M; Karahalil B; Sentürker S; Buckley TJ; Roldán-Arjona T Excision of Products of Oxidative DNA Base Damage by Human NTH1 Protein. Biochemistry 1999, 38 (1), 243–246. 10.1021/bi9819071. [PubMed: 9890904]

(45). Albelazi MS; Martin PR; Mohammed S; Mutti L; Parsons JL; Elder RH The Biochemical Role of the Human NEIL1 and NEIL3 DNA Glycosylases on Model DNA Replication Forks. Genes (Basel). 2019, 10 (4). 10.3390/genes10040315.

(46). Leipold MD; Workman H; Muller JG; Burrows CJ; David SS Recognition and Removal of Oxidized Guanines in Duplex DNA by the Base Excision Repair Enzymes HOGG1, YOGG1, and YOGG2. Biochemistry 2003, 42 (38), 11373–11381. 10.1021/bi034951b. [PubMed: 14503888]

(47). Vaisman A; Woodgate R Unique Misinsertion Specificity of Poı May Decrease the Mutagenic Potential of Deaminated Cytosines. EMBO J. 2001, 20 (22), 6520–6529. 10.1093/emboj/20.22.6520. [PubMed: 11707422]

(48). Lukmanov T; Ivanov SP; Khamitov EM; Khursan SL Relative Stability of Keto-Enol Tautomers in 5,6-Substituted Uracils: Ab Initio, DFT and PCM Study. Comput. Theor. Chem 2013, 1023, 38–45. 10.1016/j.comptc.2013.09.005.

(49). Imamura K; Averill A; Wallace SS; Doublié S Structural Characterization of Viral Ortholog of Human DNA Glycosylase NEIL1 Bound to Thymine Glycol or 5-Hydroxyuracil-Containing DNA. J. Biol. Chem 2012, 287 (6), 4288–4298. 10.1074/jbc.M111.315309. [PubMed: 22170059]

(50). Radom CT; Banerjee A; Verdine GL Structural Characterization of Human 8-Oxoguanine DNA Glycosylase Variants Bearing Active Site Mutations. J. Biol. Chem 2007, 282 (12), 9182–9184. 10.1074/jbc.M608989200. [PubMed: 17114185]

(51). Wang L; Lee SJ; Verdine GL Structural Basis for Avoidance of Promutagenic DNA Repair by MutY Adenine DNA Glycosylase. J. Biol. Chem 2015, 290 (28), 17096–17105. 10.1074/jbc.M115.657866. [PubMed: 25995449]

(52). Kundu S; Brinkmeyer MK; Livingston AL; David SS Adenine Removal Activity and Bacterial Complementation with the Human MutY Homologue (MUTYH) and Y165C, G382D, P391L and Q324R Variants Associated with Colorectal Cancer. DNA Repair (Amst) . 2009, 8 (12), 1400–1410. 10.1016/j.dnarep.2009.09.009. [PubMed: 19836313]

(53). Lee AJ; Warshaw DM; Wallace SS Insights into the Glycosylase Search for Damage from Single-Molecule Fluorescence Microscopy. DNA Repair (Amst). 2014, 20, 23–31. 10.1016/j.dnarep.2014.01.007. [PubMed: 24560296]

(54). Perlow-Poehnelt RA; Zharkov DO; Grollman AP; Broyde S Substrate Discrimination by Formamidopyrimidine-DNA Glycosylase: Distinguishing Interactions within the Active Site. Biochemistry 2004, 43 (51), 16092–16105. 10.1021/bi048747f. [PubMed: 15610004]

(55). Jia L; Shafirovich V; Geacintov NE; Broyde S Lesion Specificity in the Base Excision Repair Enzyme HNeil1: Modeling and Dynamics Studies. Biochemistry 2007, 46 (18), 5305–5314. 10.1021/bi062269m. [PubMed: 17432829]

(56). Duclos S; Aller P; Jaruga P; Dizdaroglu M; Wallace SS; Doublié S Structural and Biochemical Studies of a Plant Formamidopyrimidine-DNA Glycosylase Reveal Why Eukaryotic Fpg Glycosylases Do Not Excise 8-Oxoguanine. DNA Repair (Amst). 2012, 11 (9), 714–725. 10.1016/j.dnarep.2012.06.004. [PubMed: 22789755]

(57). Minko IG; Vartanian VL; Tozaki NN; Coskun E; Coskun SH; Jaruga P; Yeo J; David SS; Stone MP; Egli M; Dizdaroglu M; McCullough AK; Lloyd RS Recognition of DNA Adducts by Edited and Unedited Forms of DNA Glycosylase NEIL1. DNA Repair (Amst). 2020, 85, 102741. 10.1016/j.dnarep.2019.102741. [PubMed: 31733589]

(58). Meltzer M; Long K; Nie Y; Gupta M; Yang J; Montano M The RNA Editor Gene ADAR1 Is Induced in Myoblasts by Inflammatory Ligands and Buffers Stress Response. Clin. Transl. Sci 2010, 3 (3), 73–80. 10.1111/j.1752-8062.2010.00199.x. [PubMed: 20590675]

(59). Patterson JB; Samuel CE Expression and Regulation by Interferon of a Double-Stranded-RNA-Specific Adenosine Deaminase from Human Cells: Evidence for Two Forms of the Deaminase. Mol. Cell. Biol 1995, 15 (10), 5376–5388. 10.1128/mcb.15.10.5376. [PubMed: 7565688]

(60). Maydanovych O; Beal PA Breaking the Central Dogma by RNA Editing. Chemical Reviews. American Chemical Society August 2006, pp 3397–3411. 10.1021/cr050314a. [PubMed: 16895334]

(61). Teoh PJ; An O; Chung TH; Chooi JY; Toh SHM; Fan S; Wang W; Koh BTH; Fullwood MJ; Ooi MG; de Mel S; Soekojo CY; Chen L; Ng SB; Yang H; Chng WJ Aberrant Hyperediting of the Myeloma Transcriptome by ADAR1 Confers Oncogenicity and Is a Marker of Poor Prognosis. Blood 2018, 132 (12), 1304–1317. 10.1182/blood-2018-02-832576. [PubMed: 30061158]

(62). Yang JH; Luo X; Nie Y; Su Y; Zhao Q; Kabir K; Zhang D; Rabinovici R Widespread Inosine-Containing MRNA in Lymphocytes Regulated by ADAR1 in Response to Inflammation. Immunology 2003, 109 (1), 15–23. 10.1046/j.1365-2567.2003.01598.x. [PubMed: 12709013]

(63). Anadón C; Guil S; Simó-Riudalbas L; Moutinho C; Setien F; Martínez-Cardús A; Moran S; Villanueva A; Calaf M; Vidal A; Lazo PA; Zondervan I; Savola S; Kohno T; Yokota J; De Pouplana LR; Esteller M Gene Amplification-Associated Overexpression of the RNA Editing Enzyme ADAR1 Enhances Human Lung Tumorigenesis. Oncogene 2016, 35 (33), 4407–4413. 10.1038/onc.2015.469. [PubMed: 26640150]

(64). Bhate A; Sun T; Li JB ADAR1: A New Target for Immuno-Oncology Therapy. Molecular Cell. Cell Press March 7, 2019, pp 866–868. 10.1016/j.molcel.2019.02.021.

(65). Shah SP; Morin RD; Khattra J; Prentice L; Pugh T; Burleigh A; Delaney A; Gelmon K; Guliany R; Senz J; Steidl C; Holt RA; Jones S; Sun M; Leung G; Moore R; Severson T; Taylor GA; Teschendorff AE; Tse K; Turashvili G; Varhol R; Warren RL; Watson P; Zhao Y; Caldas C; Huntsman D; Hirst M; Marra MA; Aparicio S Mutational Evolution in a Lobular Breast

Tumour Profiled at Single Nucleotide Resolution. Nature 2009, 461 (7265), 809–813. 10.1038/nature08489. [PubMed: 19812674]

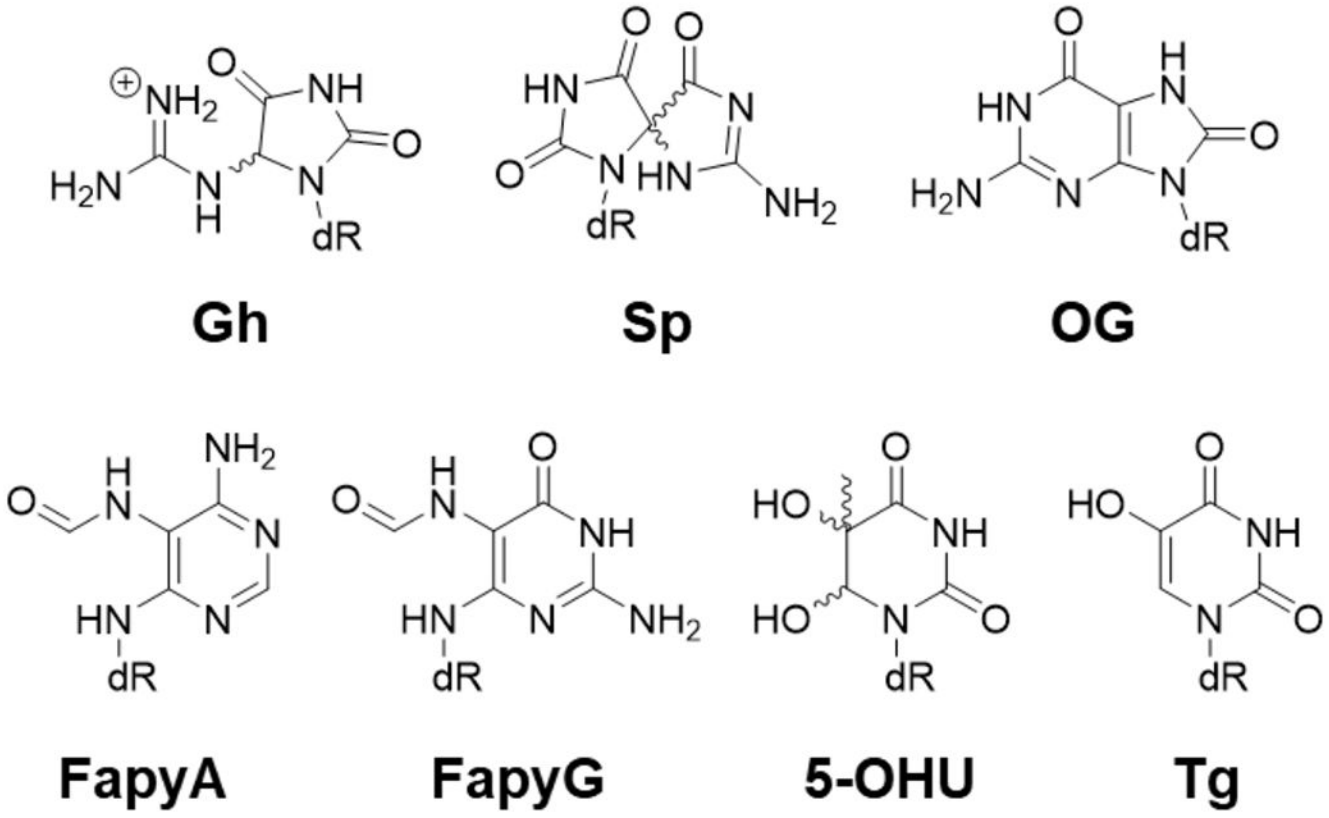

Figure 1:
Common products of oxidative base damage. All lesions except OG are substrates for NEIL1. Abbreviations (from top left to bottom right): Gh, guanidinohydantoin; Sp, spiroiminodihydantoin; OG, 8-oxo-7,8-dihydroguanine; FapyA, 4,6-diamino-5-formamidopyrimidine; FapyG, 2,6-diamino-4-oxo-5-formamidopyrimidine; 5-OHU, 5-hydroxyuracil; Tg, thymine glycol.

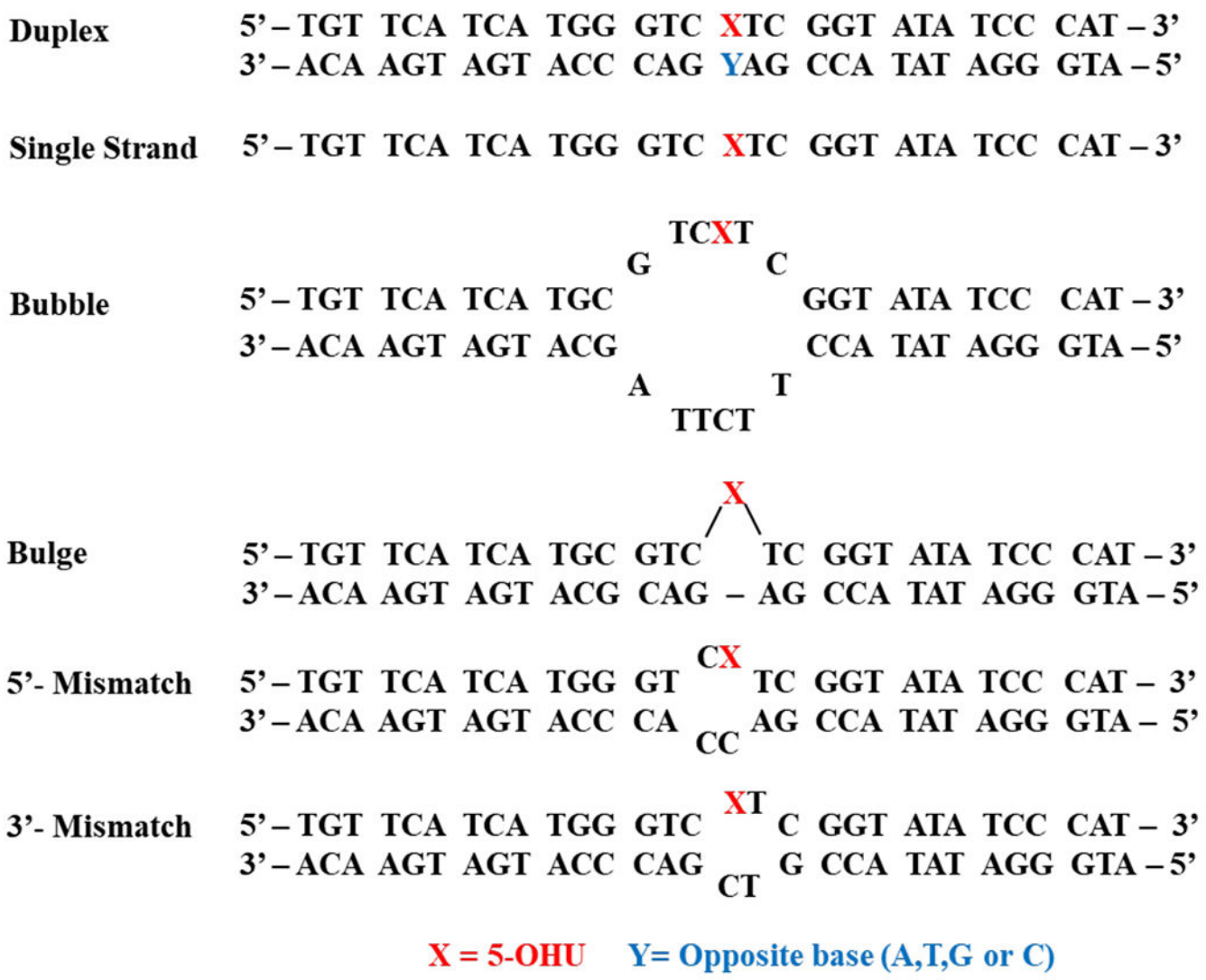

Figure 2:
DNA substrates used in this study.

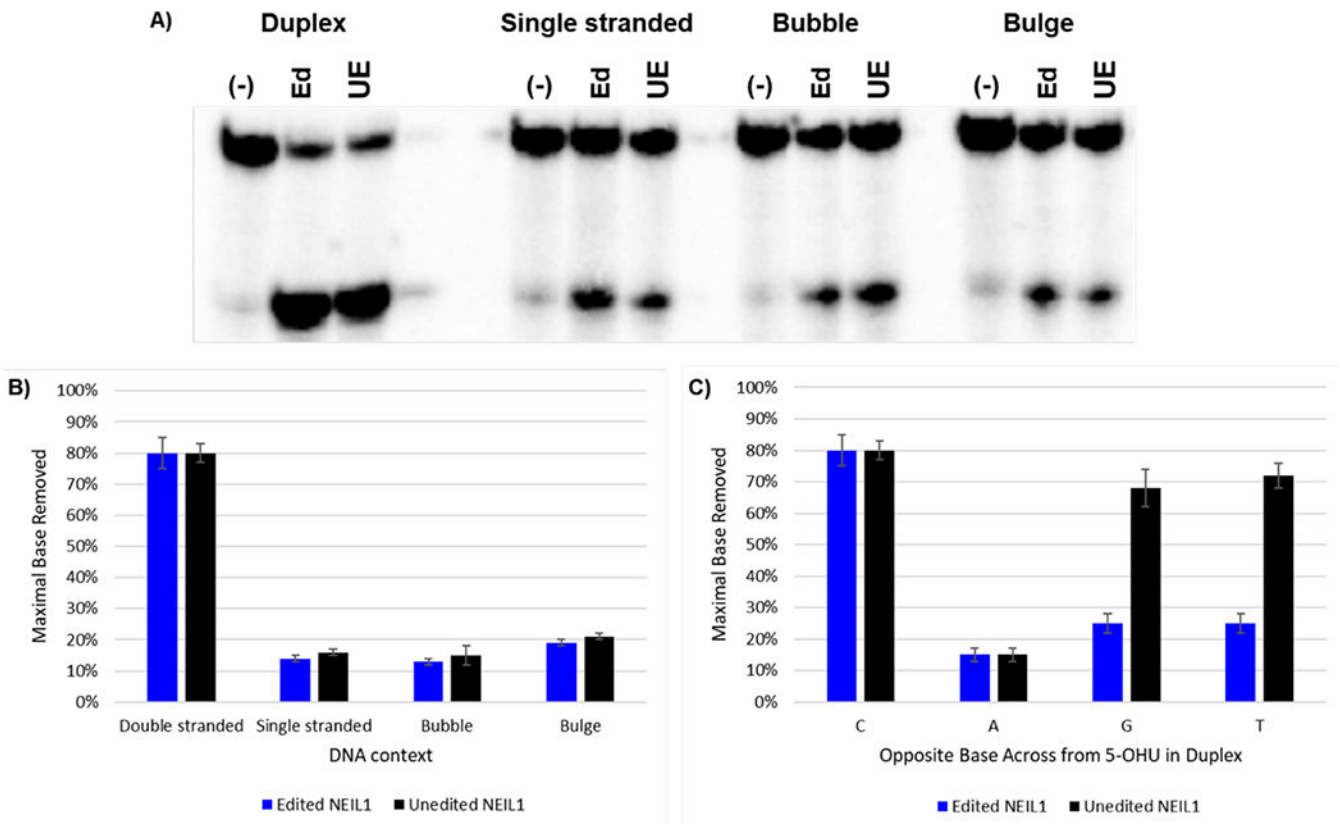

Figure 3:

Context dependence of 5-OHU removal by Edited (Ed) and Unedited (UE) NEIL1 (A) Representative gel image of Ed and UE NEIL1 5-OHU removal activity in different DNA contexts. (B) Graphical representations of extents of 5-OHU removed (%) by Ed and UE NEIL1 in different DNA contexts, with 5-OHU opposite C in duplex. (C) Graphical representations of the opposite base dependence of overall extent of 5-OHU removed by NEIL1 isoforms. 5-OHU-containing DNA duplex substrate (20 nM) was incubated with excess Ed or UE NEIL1 (200 nM) at 37°C, pH 7.6 buffer containing 150 mM NaCl. The maximal percent 5-OHU removed was calculated by dividing the concentration of product produced after a 1 hr reaction by the total concentration of substrate and multiplying by 100. Error bars are the standard error for the end-point across three trials.

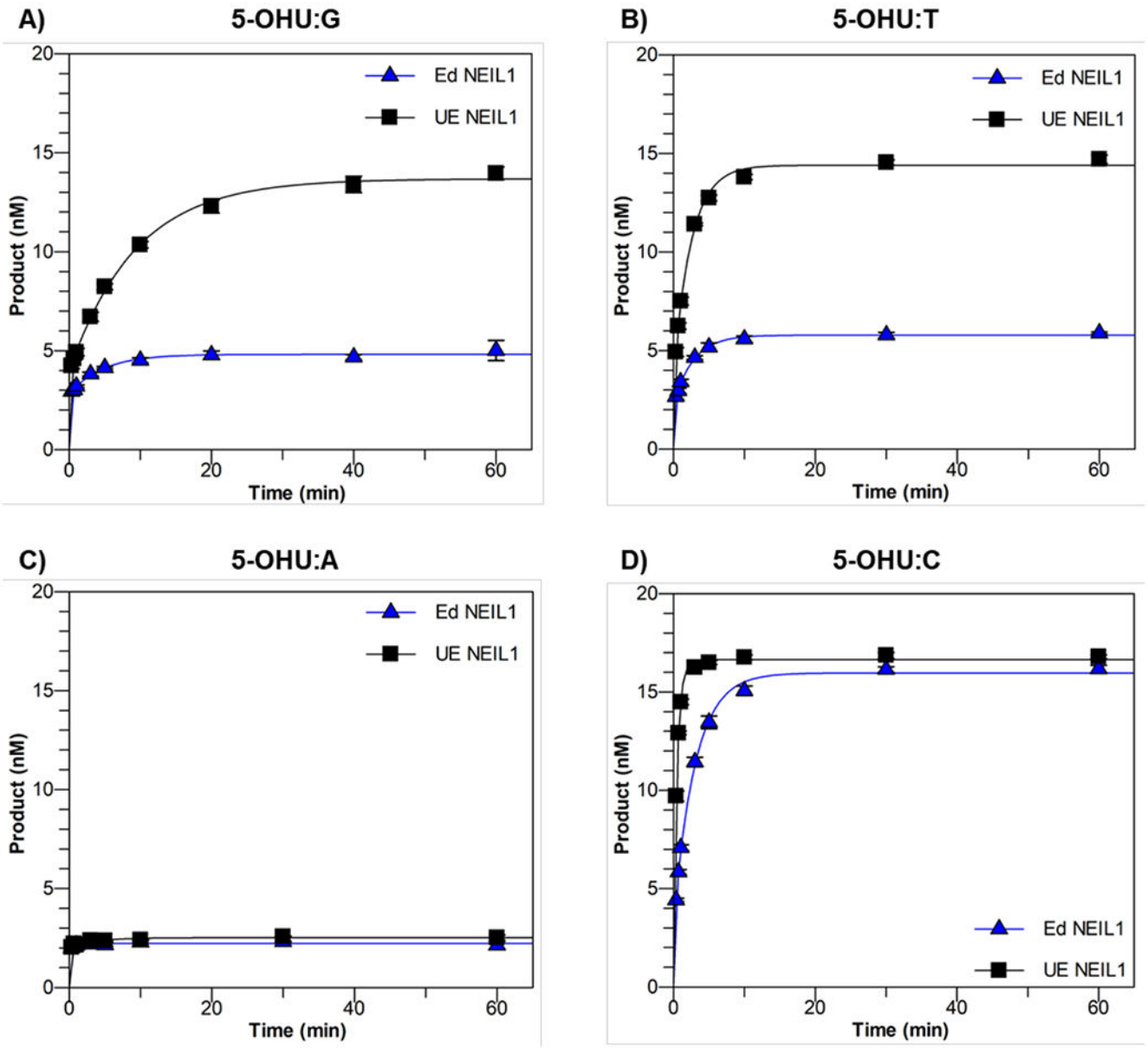

Figure 4:

Opposite base dependence of 5-OHU removal by edited (Ed) and unedited (UE) NEIL1. (A)-(D) Representative plots of product formation as a function of time under single turnover conditions with Ed and UE NEIL1 on a DNA duplex containing (A) 5-OHU:G, (B) 5-OHU:T, (C) 5-OHU:A, and (D) 5-OHU:C. 20 nM substrate was incubated with 200 nM enzyme at 37°C, pH 7.6 in the presence of 150 mM NaCl. Data is fit to a two-exponential equation, $[P]_t = A_0(1\text{-}\exp(-k_g' t)) + B_0(1\text{-}\exp(-k_g'' t))$, and the values are reported in Table 1. Error bars are the standard error for each time point across the three trials performed.

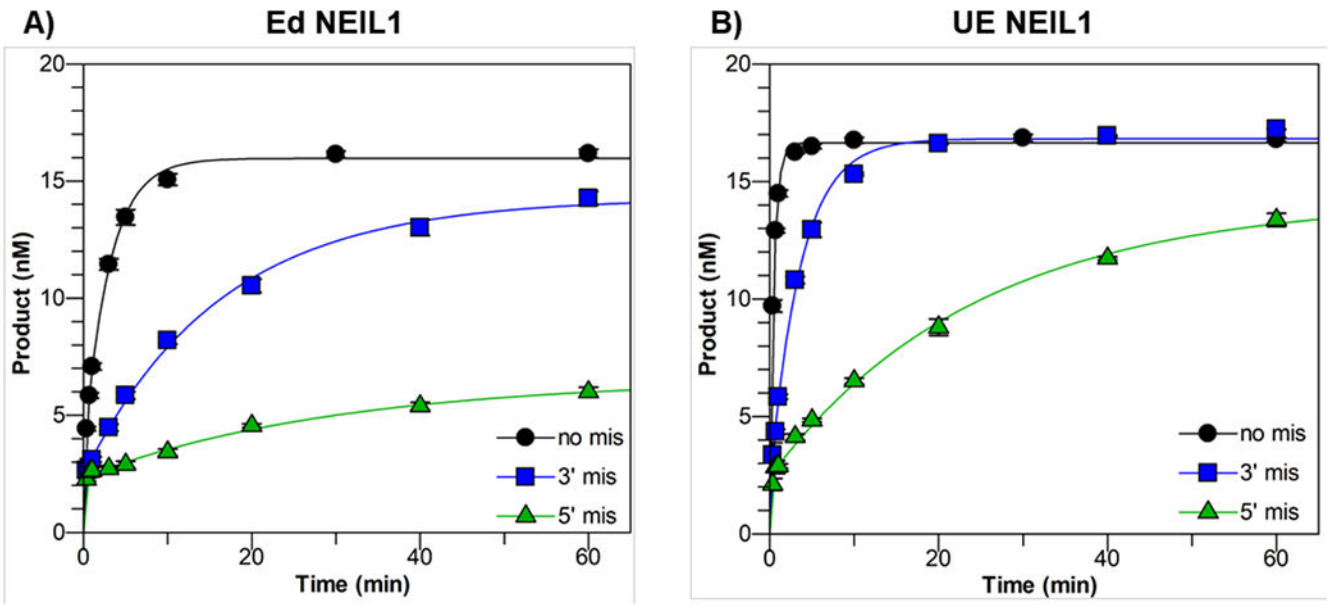

Figure 5:

Adjacent mismatches reduced efficiency of 5-OHU removal by Edited (Ed) and Unedited (UE) NEIL1. The removal of 5-OHU from a 5-OHU:C containing-duplex containing a 5' C-C mismatch or a 3' T-T mismatch to the lesion bp by A) Ed and B) UE NEIL1. [Enzyme]= 200 nM, [DNA] = 20 nM, 150 mM NaCl, pH 7.6, 37 °C, fit to a two-exponential equation, $[P]_t = A_0(1\text{-}\exp(-k_g't)) + B_0(1\text{-}\exp(-k_g''t))$. The values for k_g', k_g'', A_0, B_0, and % base removed are compiled in Table 2. Error bars are the standard error for each time point across the three trials performed.

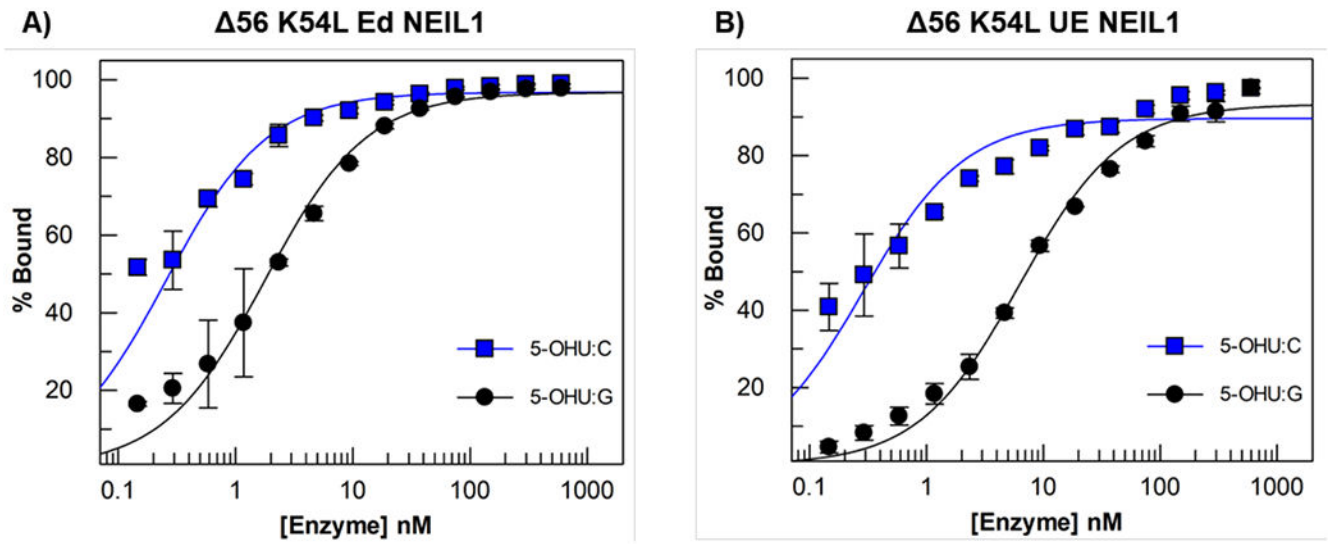

Figure 6:

Electrophoretic mobility shift assays for (A) Δ56 K54L Edited (Ed) NEIL1 and (B) Δ56 K54L Unedited (UE) NEIL1 with duplexes containing 5-OHU:C and 5-OHU:G. Duplex DNA containing a 5'-[^{32}P]-phosphate (10 pM) was incubated with the enzyme (600–0.15 nM) in buffer containing 10 % glycerol, 0.1 mg/mL BSA, 20 mM Tris pH 7.6, 150 mM NaCl, and 1 mM EDTA at 25 °C for 30 min prior to gel electrophoresis. The values for K_d are reported in Table 3. Error bars are the standard error for each concentration across the three trials performed.

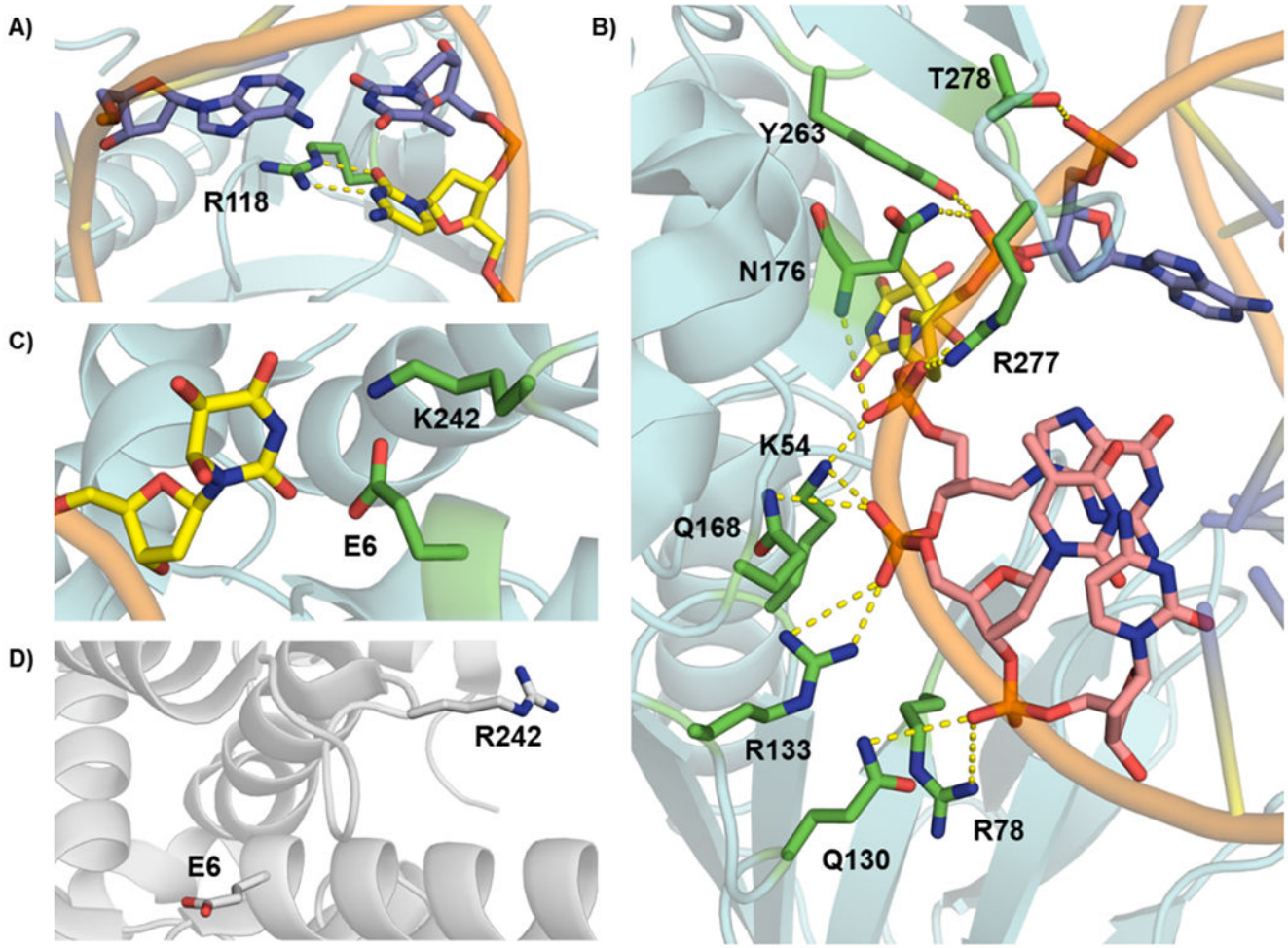

Figure 7:

NEIL1 X-ray structures reveal key amino acid residues. (A) R118 interacts with orphan base C (yellow) in the structure of P2G unedited (UE) NEIL1 bound to Tg:C-containing duplex (PDB ID: 5ITX- chain A). (B) P2G UE NEIL1 (5ITX – chain A) makes extensive contacts with the phosphodiester backbone of DNA 5' and 3' to damaged Tg lesion (yellow). Seven resides (K54, R78, Q130, R133, Q168, N176, and R277) make contacts with phosphodiester backbone 3' (peach) and three residues (N176, Y263, and T278) make contacts 5' (purple) to Tg, respectively. (C) Conformation of the loop containing residue 242 observed in the X-ray structure of P2G UE NEIL1 bound to Tg-containing DNA (5ITX-chain A) that positions residue 242 to interact with N3 of the Tg lesion. Of note, the loop containing residue 242 is significantly disordered in all of the DNA bound crystal structures consistent with the flexibility of this region.[30] (D) X-ray crystal structure of Ed NEIL1 (1TDH) with residues R242 and E6 shown. R242 is pointing away from the lesion and is far from other catalytic residues such as E6 in the absence of DNA.

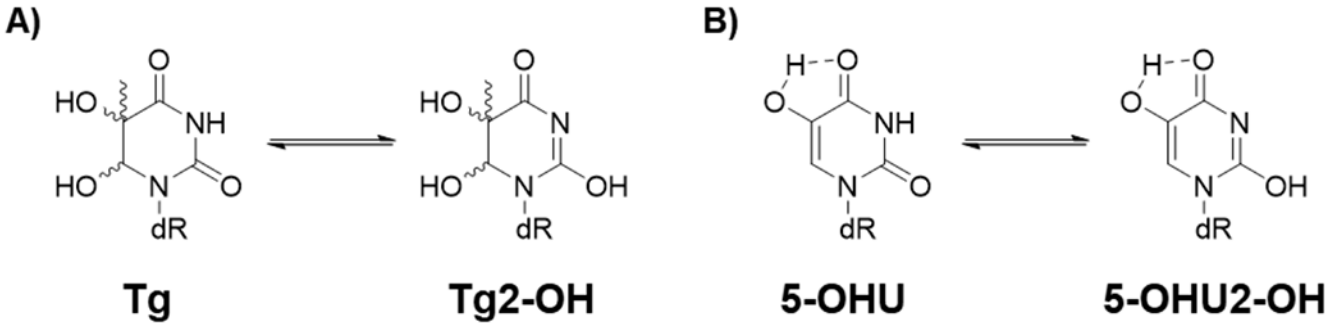

Figure 8:

Proposed tautomerization of Thymine glycol (Tg) and 5-hydroxyuracil (5-OHU). (A) Zhu *et al.* (2016) suggest that interaction with NEIL1 produces the enol tautomer Tg2-OH. The tautomer at N3 and C2 is proposed to have more favorable interactions in the NEIL1 active site.[30] (B) Proposed tautomer of 5-OHU where hydrogen bonding between the OH on C5 and oxygen C5 stabilizes the enol.[48]

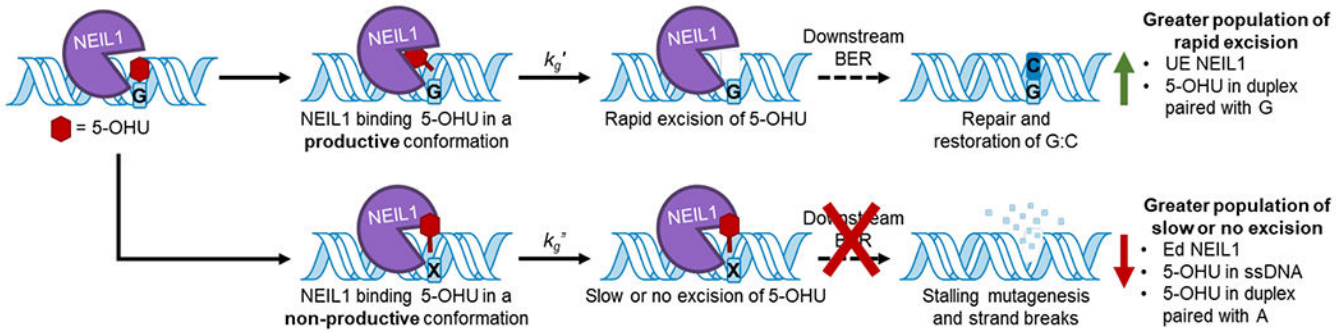

Figure 9:

NEIL1 binding and excision of 5-hydroxyuracil (5-OHU). The 5-OHU lesion will be initially identified by either Ed or UE NEIL1. The 5-OHU lesion will then be extruded from the DNA helix into the NEIL1 active site in a productive conformation for catalysis or into an alternative non-productive site and/or conformation that does not lead to excision. Recognition of 5-OHU:G bps and productive engagement of 5-OHU in the active will lead to rapid excision of 5-OHU and restoration of the original C:G bp. In contrast, non-productive placement and positioning of 5-OHU by NEIL1 leads to slow or stalled excision of 5-OHU, which may prevent mutagenesis or strand breaks in contexts such as 5-OHU:A bps and ss DNA.

Table 1.

Opposite base dependence of 5-OHU removal by Ed and UE NEIL1.

Enzyme	Base opposite 5-OHU	k_g' (min^{-1})	Capacity (A)	k_g" (min^{-1})	Capacity (B)	Total base excised (%)
Ed NEIL1	G	> 2	2.8 ± 0.4	0.22 ± 0.09	2.0 ± 0.2	24 ± 3
	C	> 2	3.3 ± 0.7	0.33 ± 0.08	13 ± 1.0	80 ± 5
	A	> 2	2.0 ± 0.4	0.7 ± 0.1	0.3 ± 0.1	11 ± 2
	T	> 2	2.3 ± 0.4	0.4 ± 0.1	3.5 ± 0.3	27 ± 3
UE NEIL1	G	> 2	4.0 ± 0.4	0.11 ± 0.04	9.7 ± 0.3	68 ± 6
	C	> 2	4.2 ± 0.2	1.8 ± 0.2	12 ± 0.2	83 ± 3
	A	> 2	2.1 ± 0.2	0.27 ± 0.07	0.5 ± 0.1	12 ± 2
	T	> 2	3.7 ± 0.4	0.4 ± 0.1	11 ± 0.3	72 ± 4

Rate constants of 5-OHU removal (min^{-1}), the associated amplitude of each rate constant (capacity, nM), and percent 5-OHU removed after 60 min incubation. [Enzyme]= 200 nM, [DNA] = 20 nM, pH 7.6, 37 °C, fit to a two-exponential equation, $[P]_t = A(1\text{-}exp(-k_g't)) + B(1\text{-}exp(-k_g''t))$. Total 5-OHU excised (%) = ((A+B)/20)*100. Data represented is an average of a minimum of 3 data sets and standard error is calculated from fits across each data set.

Table 2:

The effect of adjacent mismatches on the removal of 5-OHU opposite C by Edited (Ed) and Unedited (UE) NEIL1.

	Mismatch	k_g' (min^{-1})	Capacity (A)	k_g" (min^{-1})	Capacity (B)	Total base excised (%)
Ed NEIL1	3'	> 2	2.4 ± 0.2	0.06 ± 0.01	11.8 ± 0.4	71 ± 2
	5'	> 2	2.4 ± 0.2	0.03 ± 0.01	4.2 ± 0.4	33 ± 2
	No	> 2	3.4 ± 0.4	0.30 ± 0.02	12.6 ± 0.4	80 ± 3
UE NEIL1	3'	> 2	2.2 ± 0.4	0.30 ± 0.02	14.6 ± 0.4	84 ± 3
	5'	> 2	2.4 ± 0.2	0.04 ± 0.01	11.8 ± 0.6	71 ± 3
	No	> 2	4.2 ± 1.0	2.0 ± 0.2	12.6 ± 1.0	84 ±7

Rate constants of base removal (min^{-1}), the associated amplitude of each rate constant (capacity, nM) and percent 5-OHU removed after 60 min incubation. [Enzyme]= 200 nM, [DNA] = 20 nM, pH 7.6, 37 °C, fit to a two-exponential equation, $[P]_t = A(1-\exp(-k_g' t)) + B(1-\exp(-k_g'' t))$. Percent 5-OHU excised = ((A+B)/20)*100. Data represented is an average of a minimum of 3 data sets and standard error is calculated from fits across each data set.

Table 3:

Dissociation constants (K_d) for 5-OHU:C and 5-OHU:G with Δ56 K54 Edited (Ed) and Unedited (UE) NEIL1.

Duplex	Ed NEIL1 K_d (nM)	UE NEIL1 K_d (nM)
5-OHU:C	0.2 ± 0.1	0.3 ± 0.1
5-OHU:G	1.8 ± 0.6	6.3 ± 0.2

Duplex DNA containing a 5'-[^{32}P]-phosphate label (10 pM) was incubated with the enzyme (600–0.15 nM) in buffer containing 10 % glycerol, 0.1 mg/mL BSA, 20 mM Tris pH 7.6, 150 mM NaCl, and 1 mM EDTA at 25 °C for 30 min prior to gel electrophoresis. Data represented is an average of a minimum of 3 data sets and standard error is calculated from fits across each data set.